symmetry

MDPI

Article

On Differential Equation Models with Memory Effects in Epidemiology

Mieczysław Cichoń [1,*,†] and Kinga Cichoń [2,†]

[1] Faculty of Mathematics and Computer Science, Adam Mickiewicz University, Uniwersytetu Poznańskiego 4, 61–614 Poznań, Poland
[2] Faculty of Automatic Control, Robotics and Electrical Engineering, Poznan University of Technology, Piotrowo 3A, 60–965 Poznań, Poland; kinga.cichon@put.poznan.pl
* Correspondence: mieczyslaw.cichon@amu.edu.pl
† These authors contributed equally to this work.

Abstract

The paper has two main objectives. Firstly, it aims to identify appropriate fractional derivatives for epidemiological models and to investigate their advantages over ordinary derivatives, particularly in terms of the accuracy of epidemic simulations. The choice of a fractional derivative is motivated by its ability to represent the memory effects inherent in epidemiological processes. Different fractional derivatives may induce substantially different memory mechanisms; therefore, the relation between the choice of the derivative and the resulting memory effect is discussed in detail. The results are complemented by stability studies. The obtained uniqueness results provide a theoretical basis for the application of numerical methods, while numerical simulations demonstrate the impact of the fractional-order parameters. Secondly, the paper presents an SIQR epidemiological model incorporating quarantine, fractional derivatives, and multiple delays. The simultaneous use of fractional derivatives and delays makes it possible to account for both distributed memory effects and specific temporal lags within a unified model framework.

Keywords: SIQR model, epidemiology, fractional derivative, fractional integral operator, functional differential equation

MSC: 34K37; 34A08; 92D30; 34K20; 34K25; 47N20

1. Introduction

Papers on abstract fractional problems often involve weakening assumptions or generalizing boundary conditions (see, for example, [1–4]). Other studies focus on analyzing fractional-order operators, invertibility in specific function spaces, and their properties (see [5,6]). However, when examining a specific mathematical model, replacing ordinary derivatives with fractional-order derivatives should be preceded by an analysis of the benefits this brings and of which fractional derivatives actually provide a meaningful advantage in describing the underlying phenomenon. One of the main motivations for introducing fractional derivatives is their ability to incorporate memory effects, whereby the current state depends not only on the present but also on the past history of the process. Importantly, different fractional operators may induce different types and persistence of memory, depending on their kernels and parameters. Therefore, when studying a specific epidemiological model based on fractional differential equations, it is crucial to select fractional derivatives and integrals that provide an appropriate representation of the memory

Academic Editor: Zhan-Ping Ma

Received: 24 August 2026
Revised: 7 September 2026
Accepted: 16 September 2026
Published: 19 September 2026

effects inherent in the phenomenon under consideration. This can help determine whether the fractional formulation offers a genuine modeling advantage over the corresponding ordinary differential model.

In this paper, we examine how the choice of fractional derivative affects the resulting memory mechanism and, consequently, the model's ability to reproduce the dynamics of the underlying epidemiological process. We incorporate two memory mechanisms that act asymmetrically: a delay selects a prescribed past time, or a finite portion of history; fractional differentiation, on the other hand, distributes influence across the entire past.

The main novelty of this paper is the development and analysis of a unified framework that simultaneously incorporates two distinct types of memory effects: continuous distributed memory described by a generalized tempered fractional derivative with respect to a function g, and discrete memory represented by explicit time delays. We first study an abstract delayed problem in this setting and establish the corresponding qualitative properties. We then apply the framework to an epidemic model of SIQR type with three distinct epidemiological delays, where we investigate the positivity, existence, uniqueness, and stability of solutions and analyze the disease-free equilibrium.

A further feature of the framework is the role of the temporal scaling function g. We show that the interaction between g and the delays depends essentially on whether g is affine or nonlinear: an affine transformation preserves constant physical delays, whereas a nonlinear transformation generally produces time-dependent delays. This provides a natural interpretation of how generalized time scales interact with discrete epidemiological memory. For the affine case, we further obtain an explicit threshold result showing that the epidemic threshold is unaffected by the fractional memory order, the tempering parameter, and the explicit delays. Thus, these mechanisms influence the temporal evolution of the epidemic while, in the setting considered here, leaving the disease-free threshold unchanged. The combination of generalized fractional memory and multiple explicit delays, together with the analysis at both the abstract and epidemiological levels, constitutes the main contribution of this paper.

Given the relevance of the subject and the increasing number of related problems being investigated, we will use epidemiological models to illustrate the topic. Instead of developing models with additional factors ourselves, we will focus on an example that demonstrates the benefits of modeling with fractional order calculus.

The present study combines these two perspectives. Rather than treating the fractional formulation only as a modification of an existing epidemiological model, we aim to identify mathematical methods that are appropriate for the specific structure of the resulting system. Accordingly, we complement the application-oriented literature with relevant general results from fractional differential and integral equations, and use them as a basis for the analytical framework developed in this paper.

To address this problem, we focus on the studies that are most relevant to the objectives of the present paper. From this perspective, the existing literature can be viewed from two complementary directions. The first comprises studies in which fractional-order derivatives, most commonly of Caputo type [7–11], are introduced into epidemiological models to account for memory effects. These papers primarily emphasize the modeling and interpretation of memory effects in specific applications, often without incorporating additional mechanisms such as time delays. The second direction consists of more general mathematical studies of models involving fractional-order derivatives, not necessarily related to epidemiology ([12]). Such papers provide analytical and numerical tools for dealing with the nonlocality and memory effects inherent in fractional operators.

Epidemiological Models

Although the memory mechanisms discussed here are not specific to the SIQR model, they can, in principle, be incorporated into a wide range of epidemiological systems. However, we have chosen the SIQR model as a representative framework in which their complementary roles can be clearly illustrated. The SIQR model has recently been studied in relation to Coronavirus research due to its focus on people in quarantine (see [13,14]). It is important to note that the model should take into account the effect of delays and be based on differential equations with delay (see [15–18]). The virus is still present and emerging mutations are altering the parameters of the epidemic. Therefore, it is insufficient to consider the standard parameters of the model; rather, the model must be redesigned to reflect past and future epidemics. We therefore propose building a model based on an appropriate fractional order derivative. This model should encompass existing models but not be so broadly defined as to be chosen arbitrarily (a topic that will also be discussed in this paper).

Researchers are currently considering several sophisticated variations of these models to better simulate real-world disease dynamics like COVID-19, RSV, and HBV. In the context of SIR and SEIR models with time delay ([13,14,19]), researchers primarily use some categories of fractional derivatives. The choice depends on whether they need to represent singular memory (long-term heavy tails) or non-singular memory (shorter-term biological decay).

It is worth noting that this research can be used universally to modify other models (such as the SEIR model, cf. [19–21]). It can also be used to select parameters in the proposed model that are tailored to specific epidemics and virus types. We encourage you to continue your research and conduct further simulations based on epidemiological data. In this paper, we will focus on the mathematical foundations, demonstrating how to simulate the development of various epidemics.

There must also be a clearly identifiable symptomatic phase. The disease must have a period during which the symptoms are obvious enough to enable individuals to be identified and quarantined ([13] for the model with Caputo derivative and without delay, for instance). Effective quarantine: The pathogen should not be so contagious that quarantine in standard settings, such as homes or dedicated centers, is futile (e.g., extremely high airborne transmission before the onset of symptoms). Significant pre-quarantine infectiousness: There must be a period during which an infected person can spread the disease before being quarantined. It is this that makes the model distinct and useful. Public health capacity: The model assumes that a system is in place to identify and quarantine cases, making it more applicable to organized outbreak responses.

These are diseases where quarantine is a cornerstone of control: Smallpox (Variola virus) [22], SARS-CoV-1 (2002-2003) ([23], Ebola Virus Disease (EVD) [24]), or MERS-CoV ([25]). Suitable with some caveats: SARS-CoV-2 (COVID-19) or novel influenza strains (with pandemic potential) ([26]). The suggested approach to the topic should be used to model each of these cases, with the model parameters being adjusted to match the actual data.

The standard SIR model (Kermack, McKendrick [27,28]) is given by the system of ordinary differential equations:

$$\begin{aligned}\frac{dS}{dt} &= -\frac{\beta IS}{N},\\ \frac{dI}{dt} &= \frac{\beta IS}{N} - \gamma I,\\ \frac{dR}{dt} &= \gamma I,\end{aligned}$$

with the initial conditions $S(0) = S_0 > 0$, $I(0) = I_0 > 0$, $R(0) = R_0 \geq 0$. The total population $N = S + I + R$ is constant. To ensure the correctness of modeling results, it is important to take delays into account by using models based on differential equations with delay. However, in the case of fractional derivatives, this requires new research and differs from classical integer-order models.

In recent years, research into fractional-order SIR and SIQR models with time delay has expanded significantly. These models are favored because they capture memory effects (the impact of past conditions on current dynamics) and nonlocal behavior, which integer-order differential equations often miss. Recall that nonlocal integrals encode 'memory' in considered problems through an integral over the entire past history of the state. In epidemiology, the current infection rate depends on all past states, not only on a fixed delay. Memory is distributed and often long-range. It is useful when incubation/recovery times are heterogeneous, behavioral changes persist gradually, and immunity wanes continuously rather than abruptly. This, especially when combined with the inclusion of delays in the models, is what makes fractional-order models with delays so powerful in epidemiology. Therefore, we suggest paying attention not only to the behavior of delays in the epidemiological model but also to selecting an appropriate fractional derivative. It is possible to imagine using other fractional derivatives (nonlocal) with a greater number of parameters, but we recommend examining their impact on the process and their significance for describing the phenomenon in that case.

This paper focuses on improving the SIQR model. The SIQR model is a valuable tool for modeling infectious diseases for which quarantine is an effective and observable intervention strategy. It is particularly relevant to diseases for which isolating infected individuals is the main public health control measure.

Now, a short comment on the choice of a derivative used in the epidemiological models. The Caputo fractional derivative is the most widely used in research. Its dominance in epidemiology stems from a practical mathematical advantage: it allows for classical initial conditions. It uses a power-law kernel, meaning that the 'memory' of past infection levels decays slowly over time. It is the primary tool for modeling diseases with very long-range dependencies, such as the long-term progression of HIV or the long-term presence of pathogens in the environment. It should be noted that delays play an important role in epidemiological models, a topic that will be discussed in this paper. This suggests using models with nonlocal fractional derivatives. Models with local derivatives would not differ significantly from those with integer-order derivatives and would not offer any advantages when modeling these phenomena.

The derivative of a constant is zero, which aligns with physical intuition in biological systems (if a population remains constant, its rate of change should also be zero). Although the Riemann–Liouville derivative is mathematically fundamental, it is rarely used in applied SIR/SIQR models. This is because such derivatives require initial conditions in the form of 'fractional integrals', which are difficult to interpret in biological terms (it is impossible to measure a 'fractional number of people' at time zero).

The present paper builds on several ingredients developed in our previous studies, but its purpose is different. To highlight what this paper contributes in relation to previous research, we will provide a very brief summary of the previous stages of the research. In [29], we discuss the SIQR model itself, along with the role of the derivative parameters in describing the course of an epidemic and the methods for using them to achieve agreement with real-world data. We also discuss the problems associated with this.

The g-tempered fractional operator employed here was introduced earlier, and the numerical methodology used below is based on previously developed predictor–corrector schemes [30], where we introduce numerical methods for the fractional-order derivative under

consideration (partially for the fractional-order integral used, studied in [19]). We conduct an error analysis while preserving the Hölder regularity of the solutions for such equations.

Similarly, some aspects of parameter identifiability have been discussed in our earlier papers [19,29]. These results are used here as established tools rather than claimed as new contributions. This paper is therefore a consecutive-step study and concerns the qualitative analysis of models based on the derivatives under investigation, and above all, the role of parameter selection on memory effects (including for the SIQR model). The novelty of the present paper lies in their systematic integration into a delayed SIQR framework with three distinct epidemiological delays. We develop the corresponding abstract delayed problem and then establish existence, uniqueness, positivity, and stability properties for the concrete SIQR system. A further structural observation concerns the interaction between the temporal scaling function g and the delays: an affine g preserves a constant physical delay, whereas a nonlinear g transforms it into a time-dependent delay. This distinction is particularly relevant for interpreting generalized time scales in fractional epidemic models.

We would like to make one more important comment about the purpose of this paper. We strongly advise against creating papers by simply replacing one fractional derivative with another, of which there are many. The adopted model definition should include recognized derivatives, while certain properties and parameters should also be meaningful for the model and its solutions. We will provide a solution to the above problem.

2. Memory Effects

Clearly, this paper is not the first to consider the impact of incorporating memory effects into mathematical models. This is evident in most studies based on fractional-order nonlocal derivatives; however, it is often simply a consequence of using such derivatives (see, for example, [7]). The same is true in epidemiology (see, for example, [10]). In such cases, the derivative is fixed (typically the Caputo derivative) and no investigation is conducted into how the parameters of the derivative affect the model as a whole.

The second group of results relates to fractional-order calculus itself. This research involves studying and comparing fractional-order derivatives (including nonlocal ones), and it discusses various aspects of memory effects (see, for example, [8,9]). It also covers their applications (see [12]).

In this paper, we will emphasize the importance of the selection of an appropriate derivative for the chosen application so that the model reflects the observed effects in reality. We will also incorporate the effects resulting from delays into the model, as this is a different type of model that accounts for process memory and is complementary (and asymmetric in behavior) to the original model.

Since this paper focuses on the memory effects of the models under study, it is worth noting that we have established a definition of a fractional-order derivative for this purpose that fits well within this line of research. Further interesting examples of such derivatives can be found in [5,31]. To demonstrate the usefulness of fractional order calculus, we must select derivatives that significantly impact the model under study ([28,32]), enabling us to examine additional properties of solutions and achieve more accurate simulations of real-world phenomena (cf. [27,33,34]). Several studies (cf. [18,20]) suggest that the fractional derivatives are highly effective in modeling epidemic transition systems because they consider memory effects and universal features that are important for deterministic systems. Our model is always of the form

$$\mathcal{D}x(t) = f(t, x(t), x(t-\tau)) \quad , \quad x(s) = \psi(t) \ \text{ for } s \in [a-\tau, a],$$

where $t \in [a, b]$ and $\mathcal{D}x$ is a certain derivative of x (cf. also [35]). We will now justify our research in three areas: our choice of fractional derivatives in the model; how we determine

the usefulness of derivatives; and the mathematical difficulties this causes, as well as the differences from integer-order models. When the differential operator is nonlocal, the entire past is incorporated into the solution operator. Figures 1 and 2 illustrate this type of memory.

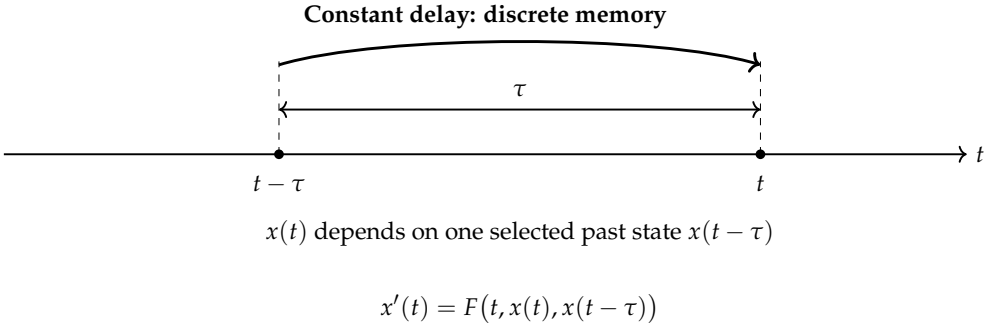

Figure 1. A constant delay produces localized memory through one selected past state $x(t-\tau)$.

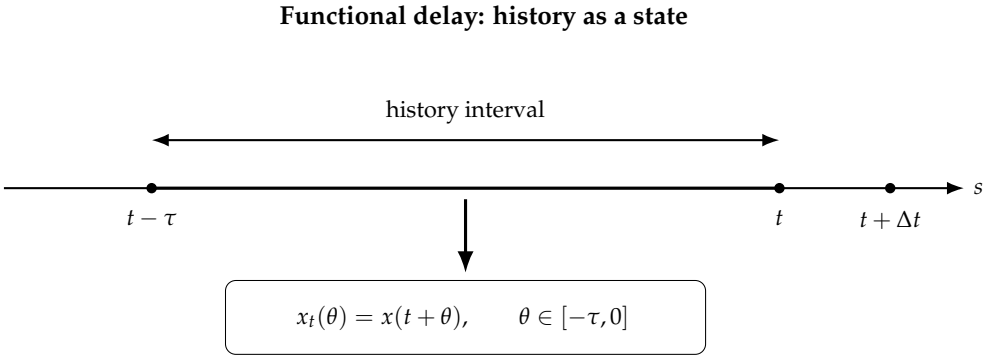

Figure 2. Functional delay as a history-dependent state. At time t, the segment $x_t(\theta) = x(t+\theta)$, $\theta \in [-\tau, 0]$, represents the recent history of the process and is treated as the current state.

In the considered models we have both fractional memory (distributed, long-range) and discrete delay memory (fixed lag τ). They do not replace each other; instead, they stack. We cannot absorb the discrete delay into the fractional kernel unless we take a singular limit.

These memory mechanisms (see Figure 3) can be extended according to the specific properties of differential operators. Their nonlocality is merely the minimum requirement. Later in this paper, we will demonstrate how we can manipulate the passage of time, among other things. After introducing the relevant fractional-order derivatives, we will revisit this topic.

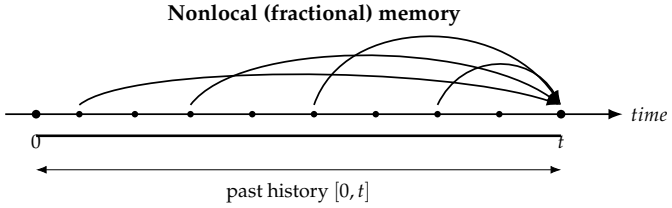

Figure 3. Schematic representation of nonlocal fractional memory. In contrast to a discrete delay, which selects a prescribed past time, a fractional derivative incorporates contributions from the entire past history $[0, t]$, with their influence determined by a nonlocal memory kernel.

Why it is important in epidemiology? Fractional delay models remember everything in the past via the fractional (nonlocal) derivatives and one specific moment via $x(t-\tau)$ ([36]). In epidemiology, the fractional part describes the heterogeneity of infectious periods and delay describe the fixed incubation or reporting lag. Models based on integer derivatives are generally considered less realistic than those based on delayed differential equations. One of the main reasons for this is the consideration of the memory effect ([37]). If we also consider the nonlocality effect of fractional derivatives, these models will achieve their full potential. Of course, this comes with certain limitations.

It is worth mentioning that our proposed approach is particularly effective in the context of fractional delay differential equations. The model described below is based on Caputo-type derivatives. What makes this model more interesting? While delays are explicit and discrete (e.g., $x(t-\tau)$), fractional derivatives also provide an implicit continuum of delays. Adding an explicit delay to a fractional model does not localize memory; rather, it creates an additional memory spike on top of an already long-tailed past.

What methods are used? The classical method of steps fails. We will prove the existence of solutions using the fixed-point method. Using the same method, although with the additional consideration of the regularity of the solutions, we will also prove their uniqueness. We will then apply numerical methods. These methods require recording the entire history and evaluating the terms based on these recorded values.

Remark 1. *A brief explanation is needed of how memory effects will manifest in the models under study. For instance, numerical simulations have shown that, when the biological model parameters are fixed, the dynamics of the solutions vary depending on the dynamic parameters of the derivative operator. This makes it possible to fit these parameters to empirical data much more accurately.*

3. Fractional Tempered Calculus

We will now identify the fractional-order derivative operators that ensure mathematical models yield realistic simulation results. The number of derivative parameters should encompass the key elements of process dynamics, including the memory effect, and enable these parameters to be determined based on empirical data (the identifiability problem).

We will now explain which fractional derivatives (see, for example, [31]) are useful in our models, although this is not an exhaustive list. We will also explain which derivatives definitely do not preserve some of the information studied in such models.

Generalized fractional tempered integral and differential operators are extensions of classical fractional calculus that incorporate an exponential tempering factor, making them particularly useful for modeling processes with memory that decays exponentially. Classical fractional derivatives/integrals (like Riemann–Liouville or Caputo) have power-law kernels [31] (e.g., $t^{\alpha-1}$), which model processes with long-range memory or heavy-tailed waiting times . However, in many real-world phenomena (e.g., finance, viscoelasticity with cutoff, anomalous diffusion in confined systems), the memory or waiting-time distribution has a power-law decay that is truncated or tempered exponentially for large times.

Fractional derivatives are appropriate when disease progression exhibits long-term memory, waiting times are non-exponential, and the effects of past interventions on current dynamics are continuous. This provides more accurate predictions about the course of the epidemic, ensuring a highly precise description of its dynamics. Taking delays into account also improves the applicability of the model. We will study the following general class of operators introduced in [1]:

Definition 1 ([1,38]). *Let $g \in C^1([a,b])$ be a positive increasing function such that $g'(t) \neq 0$, for all $t \in (a,b)$. The generalized fractional (or briefly g-fractional) integral of a function $x : [a,b] \to E$ of order $\alpha > 0$ and parameter $\mu \in \mathbb{R}^+$ is that defined by*

$$I_{a,g}^{\alpha,\mu}x(t) = \frac{1}{\Gamma(\alpha)}\int_a^t (g(t)-g(s))^{\alpha-1}e^{-\mu(g(t)-g(s))}x(s)g'(s)\,ds, \tag{1}$$

where $-\infty \le a < b \le \infty$. *For completeness, we define* $I_{a,g}^{\alpha,\mu}x(a) = 0$.

This type of fractional calculus is known as 'g-fractional calculus', and the corresponding integrals and derivatives are referred to as 'g-fractional integrals' or 'fractional integrals with respect to a function' (also known as 'ψ-fractional integrals') (see, for example, [5,38]). The advantages of models based on this type of integral (and derivative) are well recognized and have been extensively developed. Those interested will find interesting results and applications in [39–41], among others. However, due to the broad scope of the subject, this paper will concentrate on the parameters of the integral and derivative, and their role in epidemiological applications. Other aspects of this calculus are left for interested readers to explore.

Recall, in the context of epidemiological models, that α controls memory depth, i.e., smaller α implies stronger long-range memory. Both the properties of this fractional integral and all its parameters are useful in modeling real phenomena within the SIQR model.

Remark 2. *This raises questions about the problems associated with this type of situation in epidemiology. Mathematical models of epidemics should consider the various factors affecting their rate of spread. Generally, certain parameters are assumed to be constant to simplify the equations' overall form. However, the proposed model allows us to consider all factors affecting the rate of disease development by adjusting the passage of time through the g function. These functions and other parameters can be selected in simulations to ensure consistency with real-world data for different diseases and environments. This simulation example will complement the results of this research.*

Physically, if $g(t)$ *represents a 'transformed time' (e.g., disease transmission time during an epidemic, operational time in subdiffusion [42]), then this operator models tempered fractional dynamics in that transformed time. The tempering is in g-differences, not necessarily in real time* $t - s$.

The tempering factor $e^{-\mu t}$ ($\mu > 0$) *is introduced to make integrals convergent for a wider class of functions. Moreover, model memory that fades exponentially after a power-law regime and it allows better alignment with experimental data showing crossover from anomalous to normal behavior.*

Generalized fractional tempered operators are a flexible tool extending fractional calculus by incorporating an exponential tempering factor $e^{-\mu t}$ in the kernel and allowing the kernel to be a general function (not just power-law). They interpolate between classical fractional operators ($\mu = 0$) and classical integer-order operators ($\mu \to \infty$ under scaling), and they are essential for modeling processes with truncated or exponentially damped memory effects . The 'generalized' aspect allows adaptation to specific applications through kernel choice.

We propose an approach via the generalized fractional operators. It can combine two known concepts: g-fractional integrals (also called fractional integrals with respect to another function, or Kilbas–Saigo–Saxena-type integrals) and tempered fractional integrals (with the exponential tempering factor).

Consider the following integral operator ([1,5,31]):

$$I_{a,g}^{\alpha,\mu}x(t) = \frac{1}{\Gamma(\alpha)}\int_a^t (g(t)-g(s))^{\alpha-1}e^{-\mu(g(t)-g(s))}x(s)\,g'(s)\,ds$$

for some appropriately chosen function g, which will be described later. This is a special case of generalized fractional integrals with Sonine kernels, where the kernel is given by

$$K(t,s) = \frac{1}{\Gamma(\alpha)}(g(t)-g(s))^{\alpha-1}e^{-\mu(g(t)-g(s))}g'(s).$$

We start with $g \in C^1([a,b])$, with $g'(t) > 0$. This implies strict monotonicity: $g(t)-g(s) > 0$ for $t > s$, meaning that the power $(\cdot)^{\alpha-1}$ is well-defined with no issues regarding signs. This kernel is continuous except possibly at $s = t$ when $\alpha < 1$ (weak singularity, integrability).

In fractional epidemic models, the kernel encodes how past infections influence current transmission. It must be causal, positive, and biologically plausible over long periods of time, as well as be compatible with finite populations and interventions. The paper [42] demonstrates how the choice of function g impacts the consistency of the model and explains how to leverage the benefits of fractional-order integrals. The authors' subsequent papers further explore this topic.

Let $AC_g^n([a,b]) = \left\{ f : \left(\frac{d}{dg}\right)^k f \in AC([a,b]), \quad k = 0,\ldots,n-1 \right\}$ be the subspace of the space of absolutely continuous functions $AC([a,b])$. The Caputo g-tempered fractional derivative is defined as the inverse of this integral operator.

Definition 2 ([1,19,29,31]). *For $n-1 < \alpha < n$ (where n is an integer for $0 < \alpha < 1$), the definition of the Caputo g-tempered fractional derivative is as follows:*

$$\begin{aligned}\left({}^{C}\mathcal{D}_{a,g}^{\alpha,\mu} f\right)(x) &= I_{a,g}^{n-\alpha,\mu}\left(\frac{d}{dg(x)}\right)^n f(x)\\ &= \frac{1}{\Gamma(n-\alpha)}\int_a^x (g(x)-g(t))^{n-\alpha-1}e^{-\mu(g(x)-g(t))}f_g^{(n)}(t)\,dg(t),\end{aligned}$$

where $f_g^{(n)}(t) = \left(\frac{d}{dg(t)}\right)^n f(t)$.

For $0 < \alpha < 1$, under the assumption $f \in AC_g([a,b])$, we have

$$I_{a,g}^{\alpha,\mu}\left({}^{C}\mathcal{D}_{a,g}^{\alpha,\mu} f\right)(x) = f(x) - e^{-\mu(g(x)-g(a))}f(a) - \mu I_{a,g}^{1,\mu} f(x).$$

Equivalently,

$$I_{a,g}^{\alpha,\mu}\left({}^{C}\mathcal{D}_{a,g}^{\alpha,\mu} f\right)(x) = f(x) - e^{-\mu(g(x)-g(a))}f(a) - \mu\int_a^x e^{-\mu(g(x)-g(s))}f(s)g'(s)\,ds.$$

Consequently, the corresponding inverse representation is

$$f(x) = e^{-\mu(g(x)-g(a))}f(a) + I_{a,g}^{\alpha,\mu}\left({}^{C}\mathcal{D}_{a,g}^{\alpha,\mu} f\right)(x) + \mu I_{a,g}^{1,\mu} f(x).$$

This form of derivative adheres to the traditional Caputo approach. First, it isolates the integer-order warped derivative, i.e., $\left(\frac{d}{dg(t)}\right)^n f(t)$ first, and then convolves it with a combined kernel containing both the power-law memory term $(g(x)-g(t))^{n-\alpha-1}$ and the exponential tempering factor $e^{-\mu(g(x)-g(t))}$.

Lemma 1. *Let $0 < \alpha < 1$, $\mu \geq 0$, and assume that $g \in C^1([a,\infty))$ is strictly increasing with $g'(t) > 0$. Define the g-Laplace transform by*

$$\mathcal{L}_g\{f\}(s) = \int_a^\infty e^{-s(g(t)-g(a))}f(t)\,dg(t),$$

whenever the integral exists, and denote

$$F(s) = \mathcal{L}_g\{f\}(s).$$

Let $f'_g(t) = \frac{df(t)}{dg(t)}$. *Assume that the relevant transforms exist and that*

$$e^{-s(g(t)-g(a))} f(t) \longrightarrow 0 \qquad as\ t \to \infty.$$

Then the g-Laplace transform of the Caputo g-tempered fractional derivative

$${}^{C}\mathcal{D}^{\alpha,\mu}_{a,g} f(t) = I^{1-\alpha,\mu}_{a,g} f'_g(t)$$

is given by

$$\mathcal{L}_g\left\{{}^{C}\mathcal{D}^{\alpha,\mu}_{a,g} f\right\}(s) = (s+\mu)^{\alpha-1}[sF(s) - f(a)]. \tag{2}$$

Proof. By definition, ${}^{C}\mathcal{D}^{\alpha,\mu}_{a,g} f(t) = I^{1-\alpha,\mu}_{a,g} f'_g(t)$. The g-Laplace transform of the g-tempered fractional integral satisfies

$$\mathcal{L}_g\left\{I^{\beta,\mu}_{a,g} h\right\}(s) = (s+\mu)^{-\beta}\mathcal{L}_g\{h\}(s), \qquad \beta > 0.$$

Hence,

$$\mathcal{L}_g\left\{{}^{C}\mathcal{D}^{\alpha,\mu}_{a,g} f\right\}(s) = (s+\mu)^{-(1-\alpha)}\mathcal{L}_g\{f'_g\}(s).$$

It remains to evaluate the g-Laplace transform of f'_g. Since $f'_g(t) = \frac{df(t)}{dg(t)}$, integration by parts with respect to $g(t)$ yields

$$\begin{aligned}\mathcal{L}_g\{f'_g\}(s) &= \int_a^\infty e^{-s(g(t)-g(a))} f'_g(t)\, dg(t) \\ &= \left[e^{-s(g(t)-g(a))} f(t)\right]_a^\infty + s\int_a^\infty e^{-s(g(t)-g(a))} f(t)\, dg(t).\end{aligned}$$

By the assumed decay condition, $\lim_{t\to\infty} e^{-s(g(t)-g(a))} f(t) = 0$, and therefore

$$\mathcal{L}_g\{f'_g\}(s) = sF(s) - f(a).$$

Consequently,

$$\mathcal{L}_g\left\{{}^{C}\mathcal{D}^{\alpha,\mu}_{a,g} f\right\}(s) = (s+\mu)^{-(1-\alpha)}[sF(s) - f(a)] = (s+\mu)^{\alpha-1}[sF(s) - f(a)].$$

This proves (2). □

If we need to consider a scenario in which a containment policy (e.g., a lockdown) is introduced at time T_c, then the model can be constructed using a scale function g belonging to $C([a,b])$ that is piecewise differentiable (cf. [19]):

$$g(t) = t \cdot \chi_{[a,T_c)}(t) + [T_c + k(\cdot t - T_c)] \cdot \chi_{[T_c,b]}(t),$$

where $k \in (0,1)$ represents the reduction in social activity and χ_A is a characteristic function of A.

Although $g \notin C^1([a,b])$ due to the jump in the derivative at $t = T_c$, the fractional integral $\mathfrak{I}^{\alpha,\mu}_{a,g}$ remains well-defined because g is Lipschitz continuous and strictly increasing. The term $g'(s)$ in the integral is treated in the sense of Lebesgue almost everywhere or,

more generally, by Stieltjes-type integrals (cf. [19]). More details about the proposed phase space are required, so this will be studied elsewhere.

Biological effect. The transition from $g'(t) = 1$ to $g'(t) = k$ results in a visible 'flattening of the curve' (see [19]). Since the tempered fractional operator exhibits memory, the history from the 'fast' period ($t < T_c$) continues to influence the 'slow' period ($t > T_c$), though the rate of new infections is dampened by the factor k.

Now, let us quickly review what other classical fractional-order operators are included in this definition (for more details, see also [31,38,43,44]).

(1) $I_{0,g}^{\alpha,\mu}$, for $t \in [0,1]$, with

$$g(t) = \ln(1+t) \quad \text{and} \quad \mu \in \mathbb{R}^+,$$

where $\alpha > 0$. This is the generalized version of the classical Hadamard operators. It is subject to the additional condition that $\mu = 0$ ([31]).

(2) $I_{0,t}^{\alpha,0}$, for $t \in [0,1]$: These are the classical fractional operators. They are used in classical fractional calculus, involving both the Riemann–Liouville and the Caputo derivatives ([45]).

(3) $I_{a,g}^{\alpha,\mu}$, $t \in [a,b]$, with

$$\mu \neq 0 \quad \text{and} \quad g(t) = t.$$

In this case, we obtain the tempered fractional calculus. This variant of the fractional calculus plays an important role due to the use of the exponent μ, where power laws are tempered by an exponential factor.

(4) $I_{a,g}^{\alpha,0}$, $t \in [a,b]$, with

$$g(t) = t^\rho, \quad \text{and} \quad \mu \in \mathbb{R}^+,$$

where $\alpha, \rho > 0$ and we obtain the Katugampola fractional integral operators [46]. Recall that fractional integral operators with respect to t^ρ are called the Erdélyi-Kober operators.

(5) $\rho^{-\alpha} I_{a,t}^{\alpha,\frac{1-\rho}{\rho}}$, $t \in [a,b]$, $\rho \in (0,1]$ is the generalized Hilfer proportional fractional calculus ([47]).

(6) The structure and properties of the function g also have practical significance. For example, in [42], a subdiffusion equation incorporating the Caputo fractional time derivative with respect to another function g is examined and employed to model subdiffusion in a medium with time-varying properties. In this case, the following function g is given by

$$g(t) = \frac{t}{1+Bt}[1 + A\ln(1+Ct^\gamma)],$$

for some constants A, B, C and γ and then the g-subdiffusion equation describes a transition process from subdiffusion to ultraslow diffusion. The next interesting cases are described by applying the following functions:

$$g(t) = t + \frac{t[A\ln(1+Ct^\gamma) - Bt]}{1+Bt},$$

for some constants A, B, C and D_β, or

$$g(t) = t + D_\beta t^{\beta/\alpha},$$

where D_β is an ultraslow diffusion coefficient. In this situation, we find that g-type fractional calculus has a very natural area of application when $\mu = 0$. Such kernels will be referred to as 'complex' in numerical simulations.

Remark 3. *The 'complex' kernel is of particular interest due to its structure: it enables the modeler to capture behavioral transitions. In the short term, it behaves like a standard power-law kernel, which is suitable for the initial, rapid spread of a disease. In the long term, the* $1 + Bt$ *denominator and the logarithmic term slow down the rate at which 'effective time' passes. This simulates a 'tiring' or 'saturating' memory effect, whereby the impact of very old events on the current state fades more quickly than in a pure Caputo model. This flexibility makes it more effective at fitting real-world data where the intensity of the 'memory effect' may change as an epidemic progresses and public health responses are implemented.*

The system evolves on a specific scale of 'effective time', $g(t)$. When the fractional order is small (e.g., $\alpha = 0.23$), the dynamics are dominated by the singular kernel, resulting in characteristic 'jumps' or oscillations as the system responds to the time delay τ. For the Hadamard function, however, the process is much slower. The infection spreads more gradually because the 'clock' slows down as t increases. Classic quadratic or exponential kernels accelerate the dynamics, resulting in higher infection levels within the same time interval and faster fluctuations. Finally, the composite kernel exhibits hybrid behavior, combining initial linear growth with subsequent logarithmic attenuation to allow for more nuanced modeling of memory decay. These comments will be illustrated in in the section containing numerical simulations of the paper.

Throughout the paper, we distinguish between the general role of memory effects in fractional epidemic models and the specific properties that follow from the g-tempered delayed SIQR formulation considered here. Repeated explanatory remarks are therefore kept to a minimum, while the precise mathematical assumptions and model-specific consequences are stated where they are used.

Tempered Memory Effects.

We should now explain why this form of the fractional-order derivative is interesting in terms of the memory effects it preserves. In this case the memory kernel is applied exclusively to the integer-order derivative $f_g^{(n)}(t)$ (the rate of change). The memory mechanism is based on the system looking backwards in time to accumulate information on how rates of change have behaved in the past (see Figures 4 and 5). These historical rates are weighted using power-exponential decay.

Taking advantage of the specific properties of the proposed derivative enables us to better control the memory effects and their impact on the model solutions.

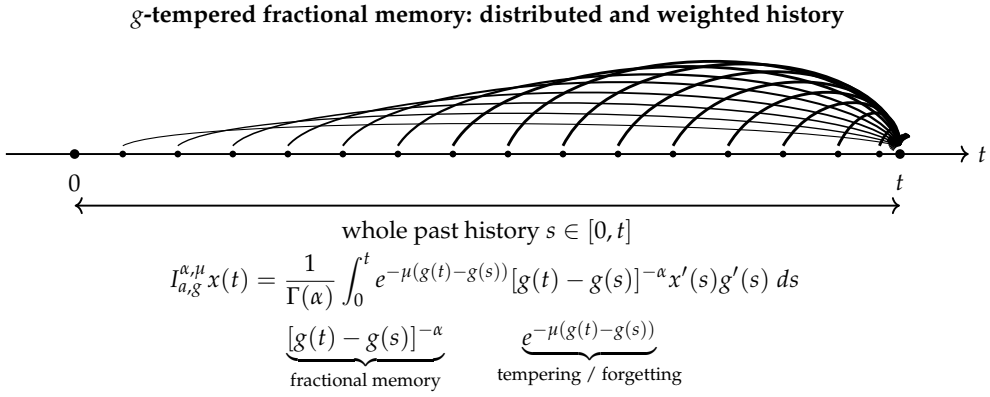

Figure 4. The g-tempered fractional derivative incorporates the whole past history, with contributions weighted according to the transformed time distance $g(t) - g(s)$. The fractional power describes the memory profile, whereas the tempering factor introduces an additional decay of the influence of the distant past.

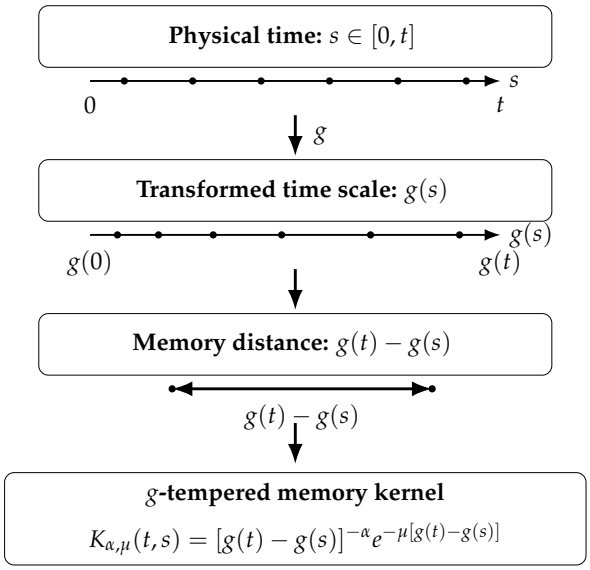

Figure 5. Schematic representation of the memory mechanism induced by a g-tempered fractional operator. The physical time s is first mapped onto the transformed scale $g(s)$. The relevant distance between the present and a past time is therefore measured by $g(t)-g(s)$, which determines the memory kernel. The fractional power describes the nonlocal memory profile, whereas the tempering parameter μ controls the decay of the influence of the distant past.

Remark 4 (Complementarity of Delay and Fractional Memory)**.** *Delay and fractional memory should not necessarily be regarded as alternative or competing mechanisms. Rather, they may represent different and complementary aspects of temporal dependence in a dynamical system.*

A delay describes a localized temporal effect associated, for example, with a finite response time, transport time, incubation period, or maturation period. In its simplest form, the current evolution depends explicitly on a prescribed past state $x(t-\tau)$. More generally, a functional delay may involve a finite segment of the recent history, represented by

$$x_t(\theta) = x(t+\theta), \qquad \theta \in [-\tau, 0].$$

Thus, delay terms identify a specific past time or a finite memory window.

The role of the function g is not merely a change in variables. It determines the time scale on which the memory of the system is measured. Fractional differentiation, in contrast, represents a distributed memory mechanism. The current evolution incorporates contributions from the entire past $s \in [0,t]$, with their influence determined by a nonlocal kernel. In the g-tempered setting, the memory is measured on the transformed time scale determined by g so that the relevant distance between the present and a past time is $g(t)-g(s)$ rather than the ordinary time difference $t-s$. The corresponding kernel contains the fractional factor

$$[g(t)-g(s)]^{-\alpha}$$

and the tempering factor

$$e^{-\mu[g(t)-g(s)]},$$

which together determine the distribution and persistence of the memory.

The two mechanisms are therefore asymmetric in their action: a delay selects a prescribed past time or a finite portion of the history, whereas fractional differentiation distributes the influence over the entire past. This difference provides a natural motivation for their simultaneous use. A delayed term can represent a well-defined lag between an event and its response, while a fractional term can describe the cumulative effect of past states that is not concentrated at any single time.

Consequently, including both mechanisms is not merely a redundant extension of the model. It allows distinct temporal scales and different types of memory to be represented simultaneously. The delay parameters determine the location or extent of the explicitly retained past, whereas the fractional parameters α, g, and μ govern how the distributed memory is measured, weighted, and attenuated. Such a combination is particularly appropriate for systems in which a specific delayed response coexists with long-range or gradually decaying memory.

However, in many applications, it is preferable to replace Caputo-type fractional derivatives with different tempered fractional derivatives. This also makes sense in the context of epidemiology, but this is a broad topic and a full discussion of it is beyond the scope of this paper. It will be discussed in a forthcoming paper. We will lay the groundwork for such generalizations by applying Stieltjes-type derivatives, which correspond to Stieltjes integral problems (see [19]). In particular, these include tempered fractional derivatives ([38]). Using the proposed derivatives will allow us to take a unified approach to these models.

4. Fractional Multiple Delay SIQR Model

As mentioned above, the fractional operator exhibits memory effects, making it useful for modeling the future state of a system based on its current state. This is evident in models for the spread of viruses (e.g., COVID-19). Using a Caputo derivative instead of a first-order derivative allows us to incorporate historical or hereditary characteristics into the model.

The following SIQR epidemic model with a single delay is considered in [14] (cf. also [48]):

$$\begin{cases} S' = \Lambda - \mu_0 S - \beta SI, \\ I' = \beta SI - \delta I - \mu_0 I - \alpha_1 I - \gamma I(t-\tau), \\ Q' = \delta I - \epsilon Q - \alpha_2 Q - \mu_0 Q, \\ R' = \gamma I(t-\tau) + \epsilon Q - \mu_0 R, \end{cases}$$

where Λ, μ_0, β, δ, γ, ϵ, α_1, and α_2 are parameters; S, I, Q, and R are control variables and τ is the time delay (see Figure 6). The descriptions of the model parameters are given in Table 1.

It will be a starting point for our discussion. Although our main objective is to select a suitable fractional derivative for epidemiological models, we will demonstrate how this model can be generalized to produce interesting solutions in various applications. We will propose taking into account fractional order derivatives, which not only formally expand the group of derivatives under study but also allow for better modeling of epidemics and the obtaining of a wide range of interesting practical results. However, our approach can also be used for other epidemiology models. This will be demonstrated within the framework of subsequent variants of this virus and in other situations where quarantine can be applied. We will generalize this model in two ways. Firstly, we will replace the standard derivatives with the fractional order derivatives proposed here. Secondly, we will consider the possibility of separate response times, or delays: τ_1 is the infection/incubation delay, τ_2 is the quarantine processing delay, τ_3 is the recovery/quarantine exit delay.

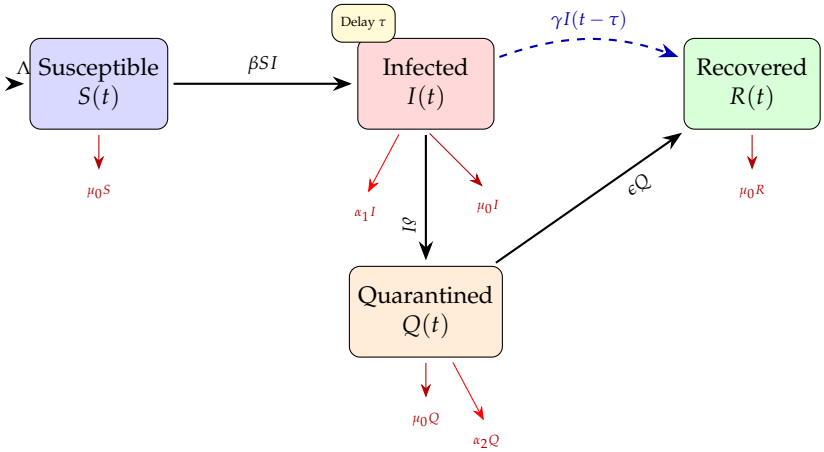

Figure 6. Flow diagram of the SIQR model with time delay.

Table 1. Definition of parameters and variables in the model.

Symbol	Definition
S	Number of susceptible people
I	Number of infected people
Q	Number of quarantined people
R	Number of recovered people
Λ	Natural increase of population
β	Transition rate from S to I
δ	Transition rate from I to Q
γ	Transition rate from I to R: cure rate of infected persons
ϵ	Transition rate from Q to R: cure rate of quarantined persons
α_1	Virus mortality rate of infected persons
α_2	Virus mortality rate of quarantined persons
μ_0	Natural death of population
τ	The time delay from infection to recovery process

The proposed model with a new derivative is not disease-specific. Rather, it reflects a basic framework for infectious diseases involving quarantine.

Remark 5. *Although the memory mechanisms discussed above—namely, explicit delays and fractional-order derivatives—can be incorporated into a wide range of epidemiological models formulated as systems of differential equations, in this paper we choose one particular model to illustrate their use and to carry out a detailed analysis. We consider the SIQR model, which provides a convenient framework for studying the interaction between delayed effects and fractional memory in an epidemiological setting.*

The choice of this model is also motivated by several recent results. For the considered SIQR formulation, existence and uniqueness of solutions and the role of the parameters of the fractional derivative in describing epidemic dynamics were investigated in [29]. Numerical methods required for the simulation of the corresponding fractional model were developed in [30], while the identifiability of the model parameters and their estimation from real data were considered in [29]. Moreover, this model admits the study of discontinuous solutions [19] (a new phase space is introduced), which is of particular interest in applications involving abrupt changes in the epidemic dynamics, such as vaccination campaigns or other intervention measures. This paper builds on and expands the research conducted on this model.

These results make the SIQR model a natural framework for the present study. Here, we complement the existing analysis by investigating the qualitative properties of solutions

for the fractional derivative adopted in this paper. In particular, since the parameters of the fractional derivative directly affect the memory mechanism and hence the resulting solutions, their role should be understood at the analytical level before interpreting the corresponding numerical simulations. The results obtained in this setting also provide a theoretical basis for applying the same fractional operator to other epidemiological models. Research on the SIQR model, which incorporates generalized, smoothed fractional derivatives and multiple delays (denoted as τ_1, τ_2, τ_3), was initiated in [19,29]. We will extend these analyses to include memory effects and qualitative analysis. We will also present the corresponding numerical simulations.

$$\begin{cases} {}^{C}\mathcal{D}^{\alpha,\mu}_{a,g} S(t) = \Lambda - \beta S(t) I(t-\tau_1) - \mu_0 S(t) \\ {}^{C}\mathcal{D}^{\alpha,\mu}_{a,g} I(t) = \beta S(t) I(t-\tau_1) + rR(t) I(t-\tau_1) - (\sigma + \mu_0) I(t) \\ {}^{C}\mathcal{D}^{\alpha,\mu}_{a,g} Q(t) = \sigma I(t-\tau_2) - (\theta + \mu_0) Q(t) \\ {}^{C}\mathcal{D}^{\alpha,\mu}_{a,g} R(t) = \theta Q(t-\tau_3) - rR(t) I(t-\tau_1) - \mu_0 R(t). \end{cases}$$

See Figure 7 for the flow diagram. Here, Λ denotes the recruitment rate, β is the effective transmission rate, and μ_0 represents the natural mortality rate. The parameter σ describes the rate of transfer of infected individuals to quarantine, while θ is the recovery rate of quarantined individuals. The parameter r characterizes the effective reinfection rate of recovered individuals. The delays τ_1, τ_2, and τ_3 represent, respectively, the transmission, quarantine, and recovery delays incorporated into the model (Table 2).

Table 2. Impact of generalized fractional tempered parameters on the SIQR model.

Parameter	Role in the Model	Impact on Solution
α	Fractional order	Dictates the 'memory' and speed of the epidemic spread via the power-law kernel.
μ	Tempering parameter	Controls the exponential decay of the memory kernel, influencing long-term behavior and stability.
$g(t)$	Scaling function	Allows for nonlinear time scales, enabling the modeling of accelerated or slowed growth phases.

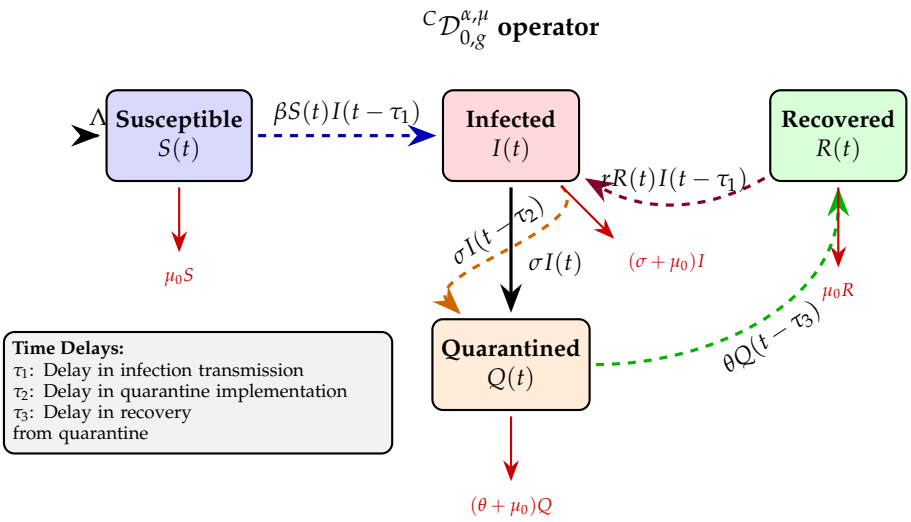

Figure 7. Flow diagram of the fractional-order SIQR model with multiple time delays and reinfection.

Because α, μ, $g(t)$, and the three delays can substantially alter the transient dynamics, their estimation from epidemic observations requires particular care. As shown in [29], the corresponding inverse problem is ill-posed and strict independent identifiability of all these parameters cannot, in general, be achieved from epidemic time-series data alone. However, when real data are used, it is possible to identify the range of interdependencies between these parameters. Consequently, the parameters affecting memory, temporal scaling, and delays should not be interpreted as independently estimable solely on the basis of the transient dynamics presented here. A detailed analysis of the resulting identifiability and parameter-compensation problems is given in [29].

When we consider some epidemiological models, our derivative has an immediate epidemiological interpretation. If $f(t)$ represents the infected population, the formula for ${}^{C}\mathcal{D}^{\alpha,\mu}_{a,g}$ shows how quickly infections were rising or falling at previous times. Accumulation is strictly based on historical changes rather than current population levels, but the distant past of infection velocity fades away exponentially. When setting up compartmental epidemic equations, this form of derivative best aligns with the natural conceptualization of epidemiological transitions. There is a clean separation of nonlinear kinetics. SIQR models rely heavily on nonlinear interaction terms on the right-hand side, such as the infection rate (βSI). This keeps the left-hand side as a clean fractional derivative of the compartment (e.g., ${}^{C}\mathcal{D}^{\alpha,\mu}_{a,g}S(t)$), enabling standard mass-action laws to be plugged in without altering the operator structure. Moreover, it has a direct epidemiological interpretation. The memory kernel acts purely on the rate of change of the compartment (e.g., how quickly infections are rising or falling). This mirrors real-world transmission dynamics, in which historical infection velocities dictate future trajectories. It is also important to note that we have known numerical methods can simulate infection peaks, quarantine capacities, and recovery curves using numerical simulations (see [30]).

Let us recall that this paper has two main objectives. First, it aims to demonstrate the advantages of using fractional derivatives in epidemiological models, such as memory effects and qualitative analysis. Second, it aims to show how various derivative parameters contribute to solutions. This will be visualized in Section 8. The parameters of the fractional operator also admit distinct epidemiological interpretations. The order α determines the strength and distribution of the nonlocal memory and may therefore affect the persistence of epidemic dynamics, including the behavior of the post-peak tail. The tempering parameter μ controls the rate at which contributions from the distant past are attenuated and hence the effective duration of the memory.

Lemma 2 (Lemma 1 in [29])**.** *For a tempered fractional system, the parameter μ defines a characteristic scale $L_\mu = 1/\mu$ known as the memory horizon. For $u \ll L_\mu$, the system is dominated by α. For $u \gg L_\mu$, the system is dominated by μ.*

Finally, the function g determines the time scale on which the fractional memory is measured, linking the internal temporal dynamics of the model with calendar time. Its choice may be informed by changes in epidemiological conditions, such as interventions, mobility, quarantine measures, or contact patterns. In our multiple-delay model we introduce the following three fixed delays: τ_1 (infection/incubation delay), τ_2 (quarantine processing delay), and τ_3 (recovery/quarantine exit delay).

The initial conditions for $t \in [-\tau, 0]$, where $\tau = \max\{\tau_1, \tau_2, \tau_3\}$, are as follows:

$$S(\theta) = \phi_1(\theta), \quad I(\theta) = \phi_2(\theta), \quad Q(\theta) = \phi_3(\theta), \quad R(\theta) = \phi_4(\theta),$$

where $\phi_i \in C([-\tau, 0], \mathbb{R}_+)$.

In the context of an SIQR model, the tempered approach is often more realistic than a purely fractional one. In a pure fractional model ($\mu = 0$), an infection that occurred years ago would still theoretically influence the current infection rate. However, in a tempered model, μ represents the biological fact that, after a certain amount of time, the 'memory' of that infection (or the effectiveness of a past quarantine policy) becomes irrelevant.

Flexibility: Setting μ to 0 yields the long-memory fractional model. Setting α to 1 while keeping μ constant produces a model that behaves like a standard ordinary differential equation (ODE) with a specific decay rate.

Models based on distributed delays. The memory effect can be also formulated in terms of systems of integer-order equations with distributed delay ([14,49]). Fractional-order models often converge more slowly to the endemic equilibrium. The 'memory' acts like friction, smoothing out the oscillations. In integer-order models with distributed delays, if the delay is long enough, it can induce instability or periodic oscillations. In fractional models, increasing the order α towards 1 usually moves the system towards standard ordinary differential equation (ODE) behavior. However, the fractional nature itself tends to be more 'stable' against such oscillations.

5. Existence, Uniqueness, and Positivity of Solutions

Introduce the transformed time

$$\xi = g(t) - g(a), \tag{3}$$

and define

$$\widetilde{f}(\xi) = f\Big(g^{-1}(\xi + g(a))\Big).$$

Since $g'(t) > 0$, the transformation is one-to-one. Setting $u = g(s) - g(a)$, $dg(s) = du$, and observing that

$$\widetilde{f}'(u) = \frac{df(s)}{dg(s)},$$

we obtain

$${}^{C}\mathcal{D}^{\alpha,\mu}_{a,g} f(t) = \frac{1}{\Gamma(1-\alpha)} \int_0^{\xi} (\xi - u)^{-\alpha} e^{-\mu(\xi-u)} \widetilde{f}'(u)\, du.$$

Thus, in the transformed time scale, the operator becomes the corresponding tempered Caputo-type operator

$${}^{C}\mathcal{D}^{\alpha,\mu}_{a,g} \widetilde{f}(\xi) = I_0^{1-\alpha,\mu} \widetilde{f}'(\xi).$$

Let $\widetilde{F}(s) = \mathcal{L}\{\widetilde{f}\}(s)$. Then

$$\mathcal{L}\Big\{{}^{C}\mathcal{D}^{\alpha,\mu}_{a,g} \widetilde{f}\Big\}(s) = (s+\mu)^{\alpha-1}\Big[s\widetilde{F}(s) - \widetilde{f}(0)\Big]. \tag{4}$$

Since $\widetilde{f}(0) = f(a)$, this is consistent with the g-Laplace transform formula obtained above.

In particular, for zero initial data,

$$\mathcal{L}\Big\{{}^{C}\mathcal{D}^{\alpha,\mu}_{a,g} \widetilde{f}\Big\}(s) = s(s+\mu)^{\alpha-1}\widetilde{F}(s).$$

It is convenient to introduce the symbol

$$\Phi_{\alpha,\mu}(s) = s(s+\mu)^{\alpha-1}.$$

Notice that $\Phi_{\alpha,0}(s) = s^{\alpha}$ so that the classical Caputo case is recovered when $\mu = 0$.

For the operator

$$ {}^{C}\mathcal{D}_{a,g}^{\alpha,\mu} f(t) = \frac{1}{\Gamma(1-\alpha)} \int_a^t [g(t)-g(s)]^{-\alpha} e^{-\mu[g(t)-g(s)]} \frac{df(s)}{dg(s)}\, dg(s), $$

the standard composition rule for the classical Caputo derivative does not extend in the same form to the present tempered operator. In particular, the relation ${}^{C}\mathcal{D}_{a,g}^{\alpha,\mu} I_{a,g}^{\alpha,\mu} f = f$ does not hold in general. Therefore, the integral representation of the differential equation should be derived directly from the Laplace transform. Consider

$$ {}^{C}\mathcal{D}_{a,g}^{\alpha,\mu} x(t) = F(t). \tag{5} $$

After the transformation (3), and writing $\widetilde{F}(\xi) = F\big(g^{-1}(\xi + g(a))\big)$, equation (4) yields

$$ (s+\mu)^{\alpha-1}(sX(s) - x(a)) = \widetilde{F}(s). $$

Consequently,

$$ X(s) = \frac{x(a)}{s} + \frac{(s+\mu)^{1-\alpha}}{s}\, \widetilde{F}(s). $$

Define

$$ \widehat{q}_{\alpha,\mu}(s) = \frac{(s+\mu)^{1-\alpha}}{s}. $$

Since

$$ \frac{(s+\mu)^{1-\alpha}}{s} = (s+\mu)^{-\alpha} + \frac{\mu}{s}(s+\mu)^{-\alpha}, $$

the inverse Laplace transform gives

$$ q_{\alpha,\mu}(u) = \frac{u^{\alpha-1}e^{-\mu u}}{\Gamma(\alpha)} + \frac{\mu}{\Gamma(\alpha)} \int_0^u v^{\alpha-1} e^{-\mu v}\, dv. \tag{6} $$

Hence, under the assumptions ensuring the existence of the Laplace transforms and the inverse transform, the corresponding Volterra representation of (5) is

$$ x(t) = x(a) + \int_a^t q_{\alpha,\mu}\big(g(t)-g(s)\big) F(s)\, dg(s). \tag{7} $$

For $\mu = 0$,

$$ q_{\alpha,0}(u) = \frac{u^{\alpha-1}}{\Gamma(\alpha)}, $$

and (7) reduces to the usual Volterra representation of a Caputo fractional equation.

Remark 6. *The kernel $q_{\alpha,\mu}$ in (7) should be distinguished from the tempered fractional kernel appearing in*

$$ I_{a,g}^{\alpha,\mu} f(t) = \frac{1}{\Gamma(\alpha)} \int_a^t [g(t)-g(s)]^{\alpha-1} e^{-\mu[g(t)-g(s)]} f(s)\, dg(s). $$

The latter defines the fractional integral operator, whereas $q_{\alpha,\mu}$ is the solution kernel obtained when (5) is solved for x. This distinction is relevant for the subsequent existence, stability, and numerical analysis.

5.1. General Fractional Delay Problems

As mentioned earlier, the proposed analysis of memory effects is not limited to the SIQR model under study. First, we will introduce an abstract theory for systems of equations and then demonstrate how to apply it to the SIQR model.

Throughout this subsection, let $0 < \alpha \leq 1$, $\mu \geq 0$, and assume that $g \in C^1([a,\infty))$, $g'(t) > 0$, $\lim_{t\to\infty} g(t) = \infty$. Let $\tau_1, \ldots, \tau_m \geq 0$, $\tau_* := \max_{1\leq j\leq m} \tau_j$. For a continuous history (initial) function

$$\varphi \in C([a-\tau_*, a], \mathbb{R}^N),$$

we consider the fractional delay equation

$$ {}^{C}\mathcal{D}^{\alpha,\mu}_{a,g} X(t) = F\big(t, X(t), X(t-\tau_1), \ldots, X(t-\tau_m)\big), \qquad t \geq a, \tag{8}$$

with

$$X(t) = \varphi(t), \qquad t \in [a-\tau_*, a]. \tag{9}$$

For $0 < \alpha < 1$, recall that ${}^{C}\mathcal{D}^{\alpha,\mu}_{a,g} X = I^{1-\alpha,\mu}_{a,g} X'_g$, $X'_g(t) = \frac{dX(t)}{dg(t)}$. As we proved, the corresponding solution kernel is

$$q_{\alpha,\mu}(u) = \frac{u^{\alpha-1}e^{-\mu u}}{\Gamma(\alpha)} + \frac{\mu}{\Gamma(\alpha)} \int_0^u v^{\alpha-1} e^{-\mu v}\, dv, \qquad u > 0. \tag{10}$$

For $\alpha = 1$ we put

$$q_{1,\mu}(u) := 1.$$

Clearly,

$$q_{\alpha,\mu}(u) > 0, \qquad u > 0,$$

and, for every $T > 0$,

$$q_{\alpha,\mu} \in L^1(0,T).$$

The Volterra representation obtained in the previous section is

$$X(t) = \varphi(a) + \int_a^t q_{\alpha,\mu}\big(g(t) - g(s)\big) F\big(s, X(s), X(s-\tau_1), \ldots, X(s-\tau_m)\big)\, dg(s).$$

For $\alpha = 1$, this reduces to

$$X(t) = \varphi(a) + \int_a^t F\big(s, X(s), X(s-\tau_1), \ldots, X(s-\tau_m)\big)\, dg(s).$$

For convenience, we denote the nonlinear vector field evaluated along the solution as

$$F_X(t) := F\big(t, X(t), X(t-\tau_1), \ldots, X(t-\tau_m)\big).$$

Expanding the definition of the modified tempered fractional derivative gives

$$I^{1-\alpha,\mu}_{a,g} X'_g(t) = \frac{1}{\Gamma(1-\alpha)} \int_a^t (g(t) - g(s))^{-\alpha} e^{-\mu(g(t)-g(s))} X'_g(s)\, g'(s)\, ds = F_X(t).$$

Multiplying both sides by $e^{\mu g(t)}$ allows us to write the left-hand side as a standard (untempered) g-fractional integral:

$$I^{1-\alpha}_{a,g}\Big[e^{\mu g(s)} X'_g(s)\Big](t) = e^{\mu g(t)} F_X(t).$$

Applying the standard g-fractional integral $I^{\alpha}_{a,g}$ to both sides reduces the left-hand side to an integer-order Stieltjes integral:

$$\int_a^t e^{\mu g(s)} X'(s)\, ds = I^{\alpha}_{a,g}\Big[e^{\mu g(s)} F_X(s)\Big](t).$$

Using integration by parts on the left-hand side ($u = e^{\mu g(s)}$ and $dv = X'(s)\,ds$) and observing that $X(a) = \varphi(a)$,

$$\int_a^t e^{\mu g(s)} X'(s)\,ds = e^{\mu g(t)} X(t) - e^{\mu g(a)} \varphi(a) - \mu \int_a^t e^{\mu g(s)} X(s)\, g'(s)\,ds.$$

Equating both sides and dividing by $e^{\mu g(t)}$ yields the implicit Volterra equation:

$$X(t) - \varphi(a) e^{-\mu(g(t)-g(a))} - \mu \int_a^t e^{-\mu(g(t)-g(s))} X(s)\, g'(s)\,ds = I_{a,g}^{\alpha,\mu} F_X(t).$$

Solving this equation explicitly for $X(t)$ replaces the exponentially decaying initial term $\varphi(a)e^{-\mu(g(t)-g(a))}$ with the constant vector $\varphi(a)$, while generating the iterated integral term:

$$\begin{aligned} X(t) &= \varphi(a) + I_{a,g}^{\alpha,\mu} F_X(t) + \mu \int_a^t \Big(I_{a,g}^{\alpha,\mu} F_X(s) \Big) g'(s)\,ds \\ &= \varphi(a) + \frac{1}{\Gamma(\alpha)} \int_a^t (g(t) - g(s))^{\alpha-1} e^{-\mu(g(t)-g(s))} F_X(s)\, g'(s)\,ds \\ &\quad + \frac{\mu}{\Gamma(\alpha)} \int_a^t \left(\int_a^s (g(s) - g(\xi))^{\alpha-1} e^{-\mu(g(s)-g(\xi))} F_X(\xi)\, g'(\xi)\,d\xi \right) g'(s)\,ds. \end{aligned}$$

5.2. A Priori Estimate for Volterra Equations

We first record a standard estimate which will be used repeatedly.

Lemma 3. *Let $T > a$, let $q \in L^1(0, g(T) - g(a))$ be nonnegative, and suppose that $u : [a, T] \to [0, \infty)$, $u \in C([a, T], [0, \infty))$ satisfies*

$$u(t) \le A + B \int_a^t q\big(g(t) - g(s)\big) u(s)\, dg(s), \qquad t \in [a, T], \tag{11}$$

where $A, B \ge 0$. Then u is bounded on $[a, T]$.

More precisely, if

$$Q_T := \int_0^{g(T)-g(a)} q(u)\,du,$$

then

$$\sup_{a \le t \le T} u(t) \le A\, C_{B,q,T},$$

where $C_{B,q,T} < \infty$ depends only on B, q, and T.

Proof. Since $q \in L^1(0, g(T) - g(a))$, one can choose $\delta > 0$ to be sufficiently small such that

$$\rho := B \int_0^{\delta} q(u)\,du < 1.$$

Because g is continuous and strictly increasing, we can partition the interval $[a, T]$ into N subintervals defined by points $a = t_0 < t_1 < \cdots < t_N = T$ such that $g(t_k) - g(t_{k-1}) \le \delta$ for all $k = 1, \ldots, N$.

Let $M_k := \sup_{t_0 \le t \le t_k} u(t)$. Note that $M_k < \infty$ because u is continuous. For any $t \in [t_{k-1}, t_k]$, we split the integral in (11) into a history part and a current part:

$$\begin{aligned} u(t) &\le A + B \int_{t_0}^{t_{k-1}} q\big(g(t) - g(s)\big) u(s)\, dg(s) + B \int_{t_{k-1}}^{t} q\big(g(t) - g(s)\big) u(s)\, dg(s) \\ &\le A + B M_{k-1} \int_{t_0}^{t_{k-1}} q\big(g(t) - g(s)\big)\, dg(s) + B \left(\sup_{s \in [t_{k-1}, t_k]} u(s) \right) \int_{t_{k-1}}^{t} q\big(g(t) - g(s)\big)\, dg(s). \end{aligned}$$

Since $\int_{t_0}^{t_{k-1}} q\big(g(t)-g(s)\big)\,dg(s) \le Q_T$ and $B\int_{t_{k-1}}^{t} q\big(g(t)-g(s)\big)\,dg(s) \le \rho < 1$, we obtain

$$u(t) \le A + BQ_T M_{k-1} + \rho \sup_{s\in[t_{k-1},t_k]} u(s).$$

Taking the supremum over $t \in [t_{k-1}, t_k]$ yields

$$\sup_{t\in[t_{k-1},t_k]} u(t) \le \frac{A + BQ_T M_{k-1}}{1-\rho}.$$

Consequently, the maximum of u on the interval up to t_k satisfies

$$M_k = \max\left\{ M_{k-1}, \sup_{t\in[t_{k-1},t_k]} u(t) \right\} \le \max\left\{ M_{k-1}, \frac{A + BQ_T M_{k-1}}{1-\rho} \right\}.$$

Since $M_0 = u(a) \le A$, iterating this recurrence N times demonstrates that M_N (which is $\sup_{a\le t\le T} u(t)$) is bounded by A multiplied by a finite constant. This constant $C_{B,q,T}$ depends only on ρ, B, Q_T, and the number of partition steps N, thus completing the proof. □

5.3. Global Existence and Uniqueness: Abstract Equation

We impose the following assumptions on F.

(H1) F is continuous on

$$[a,\infty) \times (\mathbb{R}^N)^{m+1}.$$

(H2) For every $T > a$ and $R > 0$, there exists $L_{T,R} > 0$ such that

$$\begin{aligned}\|F(t,x_0,x_1,\dots,x_m) - F(t,y_0,y_1,\dots,y_m)\| \\ \le L_{T,R}\sum_{j=0}^{m}\|x_j - y_j\|\end{aligned}$$

for all

$$t \in [a,T], \qquad \|x_j\|, \|y_j\| \le R.$$

(H3) There exist constants $A, B \ge 0$ such that

$$\|F(t,x_0,\dots,x_m)\| \le A + B\sum_{j=0}^{m}\|x_j\| \tag{12}$$

for all $t \ge a$ and all $x_j \in \mathbb{R}^N$.

Theorem 1 (Global existence and uniqueness)**.** *Assume* (H1)–(H3) *and let*

$$\varphi \in C([a-\tau_*, a], \mathbb{R}^N).$$

Then problem (8)–(9) *has a unique global continuous Volterra solution*

$$X \in C([a-\tau_*, \infty), \mathbb{R}^N).$$

Moreover, on every finite interval $[a,T]$, the solution is bounded. If, in addition, the obtained solution belongs to the domain of ${}^{C}\mathcal{D}^{\alpha,\mu}_{a,g}$, then it is a classical solution of (8).

Proof. We divide the proof into local existence, uniqueness, and continuation.

Step 1: Local existence. Define the operator $\mathcal{T}$ on

$$C([a-\tau_*, a+h], \mathbb{R}^N)$$

by

$$(\mathcal{T}X)(t) = \varphi(t), \qquad t \in [a-\tau_*, a],$$

and

$$(\mathcal{T}X)(t) = \varphi(a) + \int_a^t q_{\alpha,\mu}\big(g(t)-g(s)\big) F\big(s, X(s), X(s-\tau_1), \ldots, X(s-\tau_m)\big)\, dg(s),$$

for $t \in [a, a+h]$. Choose $R > 0$ such that

$$\|\varphi(t) - \varphi(a)\| \le R/2$$

on the history interval, after replacing R if necessary. By continuity of φ and the local boundedness of F, there exists $M_R > 0$ such that

$$\|F(t, x_0, \ldots, x_m)\| \le M_R$$

whenever

$$t \in [a, a+h], \qquad \|x_j\| \le \|\varphi\|_\infty + R.$$

Since

$$\int_0^{g(a+h)-g(a)} q_{\alpha,\mu}(u)\, du \longrightarrow 0 \qquad \text{as } h \to 0^+,$$

we can choose $h > 0$ to be sufficiently small so that $\mathcal{T}$ maps the closed ball of radius R (centered at the initial history) into itself.

For X, Y in the same ball, (H2) gives

$$\begin{aligned}\|(\mathcal{T}X)(t) - (\mathcal{T}Y)(t)\| &\le L \sum_{j=0}^{m} \int_a^t q_{\alpha,\mu}\big(g(t)-g(s)\big)\, \|X(s-\tau_j) - Y(s-\tau_j)\|\, dg(s) \\ &\le L(m+1)\left(\int_0^{g(a+h)-g(a)} q_{\alpha,\mu}(u)\, du\right) \|X - Y\|_\infty.\end{aligned}$$

Choosing h to be smaller, if necessary, makes the coefficient strictly less than one. Hence $\mathcal{T}$ is a contraction. By the Banach fixed-point theorem, a unique solution exists on $[a, a+h]$.

Step 2: Uniqueness on every finite interval. Let X and Y be two solutions on $[a, T]$ that have the same history. Define $t^* = \sup\{t \in [a, T] : X(s) = Y(s) \text{ for } s \in [a, t]\}$. Assume, for contradiction, that $t^* < T$. By continuity, $X(t^*) = Y(t^*)$. Let $Z(t) = X(t) - Y(t)$. By (H2), there exists a local Lipschitz constant $L_T > 0$ along the bounded trajectories of X and Y. For $t \in [t^*, t^* + \delta]$ with $t^* + \delta \le T$, we have

$$\|Z(t)\| \le L_T \sum_{j=0}^{m} \int_{t^*}^t q_{\alpha,\mu}\big(g(t)-g(s)\big)\, \|Z(s-\tau_j)\|\, dg(s),$$

where we used the fact that $Z(s-\tau_j) = 0$ for any $s - \tau_j \le t^*$. Let $M_\delta = \sup_{s \in [t^*, t^*+\delta]} \|Z(s)\|$. Then for $t \in [t^*, t^* + \delta]$,

$$\|Z(t)\| \le L_T(m+1) M_\delta \int_{t^*}^t q_{\alpha,\mu}\big(g(t)-g(s)\big)\, dg(s) \le L_T(m+1) Q_\delta M_\delta,$$

where $Q_\delta = \int_0^{g(t^*+\delta)-g(t^*)} q_{\alpha,\mu}(u)\,du$. Choosing $\delta > 0$ to be small enough such that $L_T(m+1)Q_\delta < 1$, we obtain $M_\delta \le \rho M_\delta$ with $\rho < 1$, which forces $M_\delta = 0$. This implies $X = Y$ on $[t^*, t^*+\delta]$, contradicting the maximality of t^*. Hence $t^* = T$, and uniqueness is global.

Step 3: A priori estimate. Let $M(t) = \sup_{a-\tau_* \le r \le t} \|X(r)\|$. We will show that $M(T) < \infty$ for any $T > a$. Using the linear growth condition (12), for $t \in [a, T]$, we obtain

$$\begin{aligned}\|X(t)\| &\le \|\varphi(a)\| + \int_a^t q_{\alpha,\mu}\big(g(t)-g(s)\big)\left[A + B\sum_{j=0}^{m}\|X(s-\tau_j)\|\right] dg(s)\\ &\le \|\varphi(a)\| + AQ_T + B(m+1)\int_a^t q_{\alpha,\mu}\big(g(t)-g(s)\big)M(s)\,dg(s),\end{aligned}$$

where $Q_T = \int_0^{g(T)-g(a)} q_{\alpha,\mu}(u)\,du$.

As in the proof of Lemma 3, we can choose a sufficiently small $\delta > 0$ such that $\rho := B(m+1)\int_0^\delta q_{\alpha,\mu}(u)\,du < 1$. Partition $[a, T]$ into subintervals at points $a = t_0 < t_1 < \cdots < t_N = T$ with $g(t_k) - g(t_{k-1}) \le \delta$. For any $t \in [t_{k-1}, t_k]$, splitting the integral gives the following:

$$\begin{aligned}\|X(t)\| &\le \|\varphi(a)\| + AQ_T + B(m+1)\int_a^{t_{k-1}} q_{\alpha,\mu}\big(g(t)-g(s)\big)M(s)\,dg(s)\\ &\quad + B(m+1)\int_{t_{k-1}}^{t} q_{\alpha,\mu}\big(g(t)-g(s)\big)M(s)\,dg(s)\\ &\le \underbrace{\|\varphi(a)\| + AQ_T + B(m+1)Q_T M(t_{k-1})}_{:=C_k} + \rho M(t_k).\end{aligned}$$

Since this holds for all $t \in [t_{k-1}, t_k]$ and $M(t)$ is non-decreasing, taking the supremum yields $M(t_k) \le \max\{M(t_{k-1}), C_k + \rho M(t_k)\}$. Thus,

$$M(t_k) \le \frac{C_k}{1-\rho} = \frac{\|\varphi(a)\| + AQ_T + B(m+1)Q_T M(t_{k-1})}{1-\rho}.$$

Starting with $M(a) = \|\varphi\|_\infty$, iterating this linear recurrence N times guarantees that $M(T) = M(t_N) < \infty$. Hence, no finite-time blow-up is possible.

Step 4: Global continuation. The local contraction argument can be restarted from any time $t_0 < T$ because the solution is bounded on $[a, T]$ and, by (H2), F is Lipschitz on bounded subsets. Therefore, the maximal interval of existence cannot have a finite right endpoint. Thus, the solution exists uniquely for every $t \ge a$. □

Remark 7. *The linear growth condition (H3) in Theorem 1 is an assumption imposed on the abstract nonlinear term in order to establish a general existence result by means of the corresponding Gronwall-type estimate. It is important to note that this condition is not satisfied, in general, by the right-hand side of the SIQR system considered below, due to the presence of bilinear incidence and reinfection terms such as*

$$\beta S(t)I(t-\tau_1) \quad \text{and} \quad rR(t)I(t-\tau_1).$$

Consequently, Theorem 1 cannot be applied directly to the SIQR system. For the concrete model, we therefore establish in Theorem 4 an appropriate a priori estimate based on the total population

$$N(t) = S(t) + I(t) + Q(t) + R(t),$$

which allows us to control the solutions despite the lack of a global linear growth bound.

5.4. Positivity of Abstract Solutions

For $x = (x_1, \dots, x_N) \in \mathbb{R}^N$, write $\mathbb{R}^N_+ = \{x \in \mathbb{R}^N : x_i \geq 0,\ i = 1, \dots, N\}$.

We assume that F satisfies the following quasipositivity condition:

$$F_i(t, x_0, x_1, \dots, x_m) \geq 0 \tag{13}$$

whenever

$$t \geq a, \qquad x_j \in \mathbb{R}^N_+, \quad j = 0, \dots, m, \qquad (x_0)_i = 0.$$

Theorem 2 (Positivity)**.** *Suppose that the assumptions of Theorem 1 hold and, in addition, F satisfies the quasipositivity condition (13). If*

$$\varphi(t) \in \mathbb{R}^N_+, \qquad t \in [a - \tau_*, a],$$

then the unique global solution satisfies

$$X(t) \in \mathbb{R}^N_+, \qquad t \geq a.$$

Proof. Suppose, to the contrary, that at least one component becomes negative. Let

$$t_* = \inf\{t > a : \ X_i(t) < 0 \text{ for some } i\}.$$

By continuity,

$$X(t) \in \mathbb{R}^N_+, \qquad a - \tau_* \leq t \leq t_*,$$

and for at least one index i,

$$X_i(t_*) = 0.$$

We use the first-contact principle for the present tempered Caputo-type operator. If a scalar function y is sufficiently regular (which holds for classical solutions at $t > a$) and satisfies

$$y(s) \geq y(t_*) = 0, \qquad a \leq s \leq t_*,$$

then

$${}^C\mathcal{D}^{\alpha,\mu}_{a,g} y(t_*) \leq 0.$$

Indeed, writing

$$k(r) = r^{-\alpha} e^{-\mu r},$$

we have

$$k'(r) = -e^{-\mu r}\left(\alpha r^{-\alpha-1} + \mu r^{-\alpha}\right) < 0.$$

Performing an integration by parts in the defining Caputo integral on $[a, t_* - \varepsilon]$ and letting $\varepsilon \downarrow 0$, while noting that the boundary term $\lim_{s \to t_*^-} k(g(t_*) - g(s))y(s) = 0$ due to the regularity of the classical solution at t_*, gives

$$\begin{aligned} {}^C\mathcal{D}^{\alpha,\mu}_{a,g} y(t_*) = &-\frac{k(g(t_*) - g(a))}{\Gamma(1-\alpha)}\, y(a) \\ &- \frac{1}{\Gamma(1-\alpha)} \int_a^{t_*} \frac{\partial}{\partial s} k(g(t_*) - g(s))\, y(s)\, ds. \end{aligned}$$

Since $\frac{\partial}{\partial s} k(g(t_*) - g(s)) = -k'(g(t_*) - g(s))g'(s) > 0$, both terms on the right-hand side are nonpositive (using $y(a) \geq 0$ and $y(s) \geq 0$).

Applying this to the first component which reaches the boundary, we obtain

$$^{C}\mathcal{D}^{\alpha,\mu}_{a,g} X_i(t_*) \leq 0.$$

On the other hand, all delayed values belong to $\mathbb{R}^N_+$, and $X_i(t_*) = 0$. Hence quasipositivity yields

$$F_i\big(t_*, X(t_*), X(t_* - \tau_1), \ldots, X(t_* - \tau_m)\big) \geq 0.$$

Since the differential equation gives

$$^{C}\mathcal{D}^{\alpha,\mu}_{a,g} X_i(t_*) = F_i\big(t_*, X(t_*), X(t_* - \tau_1), \ldots, X(t_* - \tau_m)\big),$$

we obtain

$$^{C}\mathcal{D}^{\alpha,\mu}_{a,g} X_i(t_*) \geq 0.$$

Thus equality must hold.

The standard first-contact perturbation argument, replacing X_i by $X_i + \varepsilon$ and letting $\varepsilon \downarrow 0$, then excludes a crossing of the boundary under the local Lipschitz assumption. Consequently, $X_i(t) \geq 0$ for all $t \geq a$ and all i. Hence

$$X(t) \in \mathbb{R}^N_+, \qquad t \geq a.$$

□

6. Application to the SIQR Model

We now apply the preceding results to the system

$$\begin{cases} ^{C}\mathcal{D}^{\alpha,\mu}_{a,g} S(t) = \Lambda - \beta S(t) I(t - \tau_1) - \mu_0 S(t), \\ ^{C}\mathcal{D}^{\alpha,\mu}_{a,g} I(t) = \beta S(t) I(t - \tau_1) + r R(t) I(t - \tau_1) - (\sigma + \mu_0) I(t), \\ ^{C}\mathcal{D}^{\alpha,\mu}_{a,g} Q(t) = \sigma I(t - \tau_2) - (\theta + \mu_0) Q(t), \\ ^{C}\mathcal{D}^{\alpha,\mu}_{a,g} R(t) = \theta Q(t - \tau_3) - r R(t) I(t - \tau_1) - \mu_0 R(t). \end{cases} \tag{14}$$

Assume

$$\Lambda, \beta, \mu_0, \sigma, \theta, r \geq 0, \qquad \tau_1, \tau_2, \tau_3 \geq 0, \tag{15}$$

and let

$$\tau_* = \max\{\tau_1, \tau_2, \tau_3\}.$$

The initial history is assumed to satisfy

$$S(t), I(t), Q(t), R(t) \geq 0, \qquad t \in [a - \tau_*, a]. \tag{16}$$

Since the right-hand side of (14) is a polynomial in the current and delayed variables, it is locally Lipschitz. Thus, by standard arguments (as in Step 1 of Theorem 1), a unique local continuous Volterra solution exists on some maximal interval $[a, T_{\max})$. We first establish the biological well-posedness of the model by ensuring that populations remain nonnegative.

Positivity of the SIQR Solution

We now establish the positivity of solutions for our system. The proof is based on a rigorous scalar minimum principle tailored specifically for the g-tempered Caputo operator considered in this paper.

Throughout this subsection, let $0 < \alpha < 1$, $\mu \geq 0$, and assume $g \in C^1([a, T])$ with $g'(t) > 0$. We first record the following minimum principle.

Lemma 4 (Minimum principle). *Let $0 < \alpha < 1$, $\mu \geq 0$, and let $g \in C^1([a,T])$ be strictly increasing with $g'(t) > 0$. Let $y \in C^1([a,T])$ satisfy $y(a) \geq 0$, and let c in$C([a,T])$ satisfy $c(t) \geq 0$. Suppose that*

$$ {}^{C}\mathcal{D}^{\alpha,\mu}_{a,g} y(t) + c(t)y(t) \geq 0, \qquad t \in [a,T]. \tag{17}$$

Then

$$ y(t) \geq 0, \qquad t \in [a,T].$$

Proof. Suppose, to the contrary, that $y(t_1) < 0$ for some $t_1 \in (a,T]$. Since y is continuous, y attains a negative minimum on $[a,t_1]$. Let $t_* \in (a,t_1]$ be such that

$$ y(t_*) = \min_{a \leq t \leq t_1} y(t) < 0.$$

Thus, $y(t_*) \leq y(s)$ for $a \leq s \leq t_*$.
Set

$$ G = g(t_*), \qquad A = g(a), \qquad Y(z) = y(g^{-1}(z)).$$

Then $Y(G) = y(t_*) < 0$, and $Y(G) \leq Y(z)$ for $A \leq z \leq G$. By definition and integration by parts on $[A, G-\varepsilon]$ for $\varepsilon > 0$, it is convenient to rewrite the fractional derivative in terms of the difference from the minimum value. Since $Y(G) = y(t_*)$, we have

$$ \begin{aligned} {}^{C}\mathcal{D}^{\alpha,\mu}_{a,g} y(t_*) &= \frac{e^{-\mu(G-A)}(G-A)^{-\alpha}}{\Gamma(1-\alpha)}\big(y(t_*) - y(a)\big) \\ &\quad + \frac{1}{\Gamma(1-\alpha)} \int_A^G e^{-\mu(G-z)} \Big[\alpha(G-z)^{-\alpha-1} + \mu(G-z)^{-\alpha}\Big] \big(Y(G) - Y(z)\big)\, dz. \end{aligned} \tag{18}$$

The passage to the limit as $\varepsilon \to 0^+$ is justified as follows. Since $Y \in C^1([A,G])$ and $Y(G) - Y(z) = O(G-z)$ as $z \to G^-$, the boundary term at $G-\varepsilon$ tends to zero and the integrand in the second term is of order $(G-z)^{-\alpha}$ near $z = G$, which is integrable because $0 < \alpha < 1$.

Now, $y(t_*) - y(a) \leq 0$ because $y(a) \geq 0$ and $y(t_*) < 0$, while $Y(G) - Y(z) \leq 0$ because $Y(G)$ is the minimum. Moreover,

$$ e^{-\mu(G-z)} \Big[\alpha(G-z)^{-\alpha-1} + \mu(G-z)^{-\alpha}\Big] > 0.$$

Hence, looking at (18), we deduce that

$$ {}^{C}\mathcal{D}^{\alpha,\mu}_{a,g} y(t_*) < 0.$$

On the other hand, since $y(t_*) < 0$ and $c(t_*) \geq 0$, we have $c(t_*)y(t_*) \leq 0$. Therefore,

$$ {}^{C}\mathcal{D}^{\alpha,\mu}_{a,g} y(t_*) + c(t_*)y(t_*) < 0,$$

which contradicts (17). Consequently, $y(t) \geq 0$ for all $t \in [a,T]$. □

Theorem 3 (Positivity of the SIQR solution). *Under the assumptions* (15) *and* (16), *the unique local solution of* (14) *satisfies*

$$ S(t), I(t), Q(t), R(t) \geq 0, \qquad t \in [a, T_{\max}).$$

Proof. We rewrite the SIQR system in the form

$$\begin{aligned}
{}^{C}\mathcal{D}_{a,g}^{\alpha,\mu} S(t) + c_S(t)S(t) &= \Lambda,\\
{}^{C}\mathcal{D}_{a,g}^{\alpha,\mu} I(t) + c_I I(t) &= \big(\beta S(t) + rR(t)\big) I(t-\tau_1),\\
{}^{C}\mathcal{D}_{a,g}^{\alpha,\mu} Q(t) + c_Q Q(t) &= \sigma I(t-\tau_2),\\
{}^{C}\mathcal{D}_{a,g}^{\alpha,\mu} R(t) + c_R(t)R(t) &= \theta Q(t-\tau_3),
\end{aligned}$$

where

$$c_S(t) = \mu_0 + \beta I(t-\tau_1), \qquad c_I = \sigma + \mu_0,$$
$$c_Q = \theta + \mu_0, \qquad c_R(t) = \mu_0 + rI(t-\tau_1).$$

By the assumptions on the parameters,

$$c_S(t) \geq 0, \qquad c_I > 0, \qquad c_Q > 0, \qquad c_R(t) \geq 0$$

whenever the delayed infected component is nonnegative.

Suppose, to the contrary, that at least one component becomes negative. Since the history functions are nonnegative, there exists a first time $t_0 \in (a, T_{\max})$ at which one of the components attains a negative value. Denote this component by X. Then

$$X(t_0) = \min_{a \leq t \leq t_0} X(t) < 0,$$

while

$$S(t), I(t), Q(t), R(t) \geq 0, \qquad a \leq t < t_0.$$

Since $\tau_1, \tau_2, \tau_3 > 0$, all delayed values occurring at t_0 correspond to times strictly smaller than t_0 and are therefore nonnegative.

If $X = S$, then

$${}^{C}\mathcal{D}_{a,g}^{\alpha,\mu} S(t_0) = \Lambda - c_S(t_0)S(t_0) > 0,$$

because $\Lambda > 0$, $c_S(t_0) \geq 0$, and $S(t_0) < 0$. On the other hand, by Lemma 4,

$${}^{C}\mathcal{D}_{a,g}^{\alpha,\mu} S(t_0) < 0,$$

which is a contradiction.

If $X = I$, then

$${}^{C}\mathcal{D}_{a,g}^{\alpha,\mu} I(t_0) = \big(\beta S(t_0) + rR(t_0)\big) I(t_0 - \tau_1) - c_I I(t_0) > 0,$$

because

$$S(t_0), R(t_0), I(t_0 - \tau_1) \geq 0, \qquad c_I > 0, \qquad I(t_0) < 0.$$

This again contradicts Lemma 4.

If $X = Q$, then

$${}^{C}\mathcal{D}_{a,g}^{\alpha,\mu} Q(t_0) = \sigma I(t_0 - \tau_2) - c_Q Q(t_0) > 0,$$

since

$$I(t_0 - \tau_2) \geq 0, \qquad c_Q > 0, \qquad Q(t_0) < 0.$$

This contradicts the minimum principle.

Finally, if $X = R$, then

$${}^{C}\mathcal{D}_{a,g}^{\alpha,\mu} R(t_0) = \theta Q(t_0 - \tau_3) - c_R(t_0)R(t_0) > 0,$$

because

$$Q(t_0 - \tau_3) \geq 0, \qquad c_R(t_0) \geq 0, \qquad R(t_0) < 0.$$

Again, this contradicts Lemma 4.

Thus no component can become negative. Consequently,

$$S(t), I(t), Q(t), R(t) \geq 0, \qquad t \in [a, T_{\max}).$$

□

The following extension principle rigorously justifies the continuation of solutions for our specific fractional Volterra equation:

Lemma 5 (Continuation principle for the g-tempered Volterra equation)**.** *Let $\alpha \in (0,1)$, $\mu \geq 0$, and let $g \in C^1([a,\infty))$ be strictly increasing with $g'(t) > 0$. Consider the Volterra equation*

$$X(t) = X(a) + \int_a^t q_{\alpha,\mu}\big(g(t) - g(s)\big) F\big(s, X(s)\big)\, dg(s), \qquad t \in [a, T_{\max}), \tag{19}$$

where

$$q_{\alpha,\mu}(u) = \frac{u^{\alpha-1}e^{-\mu u}}{\Gamma(\alpha)} + \frac{\mu}{\Gamma(\alpha)} \int_0^u v^{\alpha-1} e^{-\mu v}\, dv.$$

Assume that $T_{\max} < \infty$, that F is continuous and locally Lipschitz with respect to X, and that

$$\sup_{t \in [a, T_{\max})} \|F(t, X(t))\| \leq L$$

for some $L > 0$. Then the limit

$$X_* := \lim_{t \to T_{\max}^-} X(t)$$

exists. Consequently, the solution can be continued beyond $T_{\max}$.

Proof. Write

$$q_{\alpha,\mu} = K_1 + K_2,$$

where

$$K_1(u) = \frac{u^{\alpha-1}e^{-\mu u}}{\Gamma(\alpha)}, \qquad K_2(u) = \frac{\mu}{\Gamma(\alpha)} \int_0^u v^{\alpha-1} e^{-\mu v}\, dv.$$

Let $a \leq t_1 < t_2 < T_{\max}$ and put

$$\Delta g = g(t_2) - g(t_1).$$

For the K_1-part,

$$\left\| \int_a^{t_2} K_1(g(t_2) - g(s)) F(s, X(s))\, dg(s) - \int_a^{t_1} K_1(g(t_1) - g(s)) F(s, X(s))\, dg(s) \right\|$$
$$\leq I_1 + I_2,$$

where

$$I_1 = \frac{L}{\Gamma(\alpha)} \int_{t_1}^{t_2} [g(t_2) - g(s)]^{\alpha-1} e^{-\mu(g(t_2) - g(s))}\, dg(s),$$

and

$$I_2 = \frac{L}{\Gamma(\alpha)} \int_a^{t_1} |k(g(t_2) - g(s)) - k(g(t_1) - g(s))|\, dg(s),$$

with

$$k(u) = u^{\alpha-1}e^{-\mu u}.$$

Since k is positive and decreasing on $(0, \infty)$,

$$I_1 \leq \frac{L}{\Gamma(\alpha)} \int_0^{\Delta g} u^{\alpha-1}\, du = \frac{L}{\Gamma(\alpha+1)}(\Delta g)^{\alpha},$$

and

$$I_2 \leq \frac{L}{\Gamma(\alpha)} \int_0^{\Delta g} u^{\alpha-1}e^{-\mu u}\, du \leq \frac{L}{\Gamma(\alpha+1)}(\Delta g)^{\alpha}.$$

Hence

$$\|Y_1(t_2) - Y_1(t_1)\| \leq \frac{2L}{\Gamma(\alpha+1)}[g(t_2) - g(t_1)]^{\alpha}. \tag{20}$$

For the K_2-part, note that

$$K_2'(u) = \frac{\mu}{\Gamma(\alpha)}u^{\alpha-1}e^{-\mu u}, \qquad u > 0,$$

and K_2' is integrable on every bounded interval. Thus, for

$$Y_2(t) = \int_a^t K_2(g(t) - g(s))F(s, X(s))\, dg(s),$$

we have for $t > a$

$$Y_2'(t) = g'(t) \int_a^t K_2'(g(t) - g(s))F(s, X(s))\, dg(s).$$

Consequently,

$$\|Y_2'(t)\| \leq L\|g'\|_{L^{\infty}([a,T_{\max}])}K_2(g(t) - g(a)),$$

and therefore

$$\|Y_2(t_2) - Y_2(t_1)\| \leq C_T(t_2 - t_1)$$

for some $C_T > 0$ depending only on $T_{\max}$.

Since $g \in C^1([a, T_{\max}])$,

$$g(t_2) - g(t_1) \leq \|g'\|_{L^{\infty}([a,T_{\max}])}(t_2 - t_1).$$

Together with (20), this yields

$$\|X(t_2) - X(t_1)\| \leq C_1(t_2 - t_1)^{\alpha} + C_2(t_2 - t_1),$$

where C_1, C_2 are finite constants. Hence X is uniformly Hölder continuous of the order α on $[a, T_{\max})$. In particular, $X(t)$ is Cauchy as $t \to T_{\max}^-$ and therefore there exists

$$X_* = \lim_{t \to T_{\max}^-} X(t).$$

Since F is locally Lipschitz in X, the local existence theorem applied at $t = T_{\max}$ with initial value $X(T_{\max}) = X_*$ provides a solution on $[T_{\max}, T_{\max} + \varepsilon)$, for some $\varepsilon > 0$. Joining this solution with the original one extends X beyond $T_{\max}$, contradicting the maximality of $T_{\max}$. □

With positivity guaranteed, we can now prove that the solution is global.

Theorem 4 (Global existence for the SIQR model)**.** *Under the assumptions* (15) *and* (16)*, the unique continuous Volterra solution of system* (14) *is global, i.e.,* $T_{\max} = \infty$*, and*

$$(S, I, Q, R) \in C([a - \tau_*, \infty), \mathbb{R}^4_+).$$

Proof. Unlike the abstract theorem, the SIQR right-hand side does not satisfy a global linear growth condition because of the bilinear terms $\beta S(t)I(t-\tau_1)$ and $rR(t)I(t-\tau_1)$. Therefore, Theorem 1 cannot be applied directly to the present system. Instead, we establish an a priori estimate by exploiting the structure of the total population.

Define the total population $N(t) = S(t) + I(t) + Q(t) + R(t)$. Adding the four equations in the SIQR system, the infection and reinfection terms cancel, yielding

$$\begin{aligned} {}^{C}\mathcal{D}^{\alpha,\mu}_{a,g} N(t) &= \Lambda - \mu_0 S(t) - \mu_0 I(t) \\ &\quad -\sigma I(t) + \sigma I(t-\tau_2) - \mu_0 Q(t) - \theta Q(t) + \theta Q(t-\tau_3) - \mu_0 R(t). \end{aligned}$$

This identity provides the key estimate needed to control the total population and, consequently, to establish global existence for the SIQR system without imposing a global linear growth condition on its nonlinear right-hand side.

By Theorem 3, the solution components are nonnegative. Thus, dropping the nonpositive terms $-\mu_0 S(t) - \mu_0 I(t) - \mu_0 Q(t) - \mu_0 R(t) - \sigma I(t) - \theta Q(t)$ yields the following differential inequality:

$${}^{C}\mathcal{D}^{\alpha,\mu}_{a,g} N(t) \le \Lambda + \sigma I(t-\tau_2) + \theta Q(t-\tau_3).$$

To handle the delay terms, let $M(t) = \sup_{a-\tau_* \le s \le t} N(s)$. Since $I(s) \le N(s)$ and $Q(s) \le N(s)$ for all $s \le t$, we have $I(t-\tau_2) \le M(t)$ and $Q(t-\tau_3) \le M(t)$. Consequently,

$${}^{C}\mathcal{D}^{\alpha,\mu}_{a,g} N(t) \le \Lambda + (\sigma + \theta) M(t).$$

Using the corresponding Volterra integral representation, we get, for any finite $t < T_{\max}$,

$$N(t) \le N(a) + \Lambda Q_t + (\sigma + \theta) \int_a^t q_{\alpha,\mu}\big(g(t) - g(s)\big) M(s)\, dg(s),$$

where $Q_t = \int_0^{g(t)-g(a)} q_{\alpha,\mu}(u)\, du$. Standard generalized Gronwall inequalities for Volterra equations imply that $M(t)$ (and hence $N(t)$) is uniformly bounded on any finite interval $[a, T_{\max})$.

Since $0 \le S(t), I(t), Q(t), R(t) \le N(t)$, every compartment is uniformly bounded on $[a, T_{\max})$. Consequently, the continuous right-hand side of the SIQR system remains bounded. By Lemma 5, the solution cannot blow up in finite time. Thus, the maximal interval of existence must be infinite, i.e., $T_{\max} = \infty$. □

7. Qualitative Analysis

Our analysis of the SIQR model motivates more general stability results for systems involving the g-tempered fractional operator. In particular, we investigate how the fractional order, the tempering parameter, and the time transformation g affect the qualitative behavior of solutions (see [50] for the Caputo derivative).

The classical Matignon criterion [51] provides a fundamental stability result for systems involving the standard Caputo derivative. However, for the g-tempered operator considered here, the structure of the characteristic equation is fundamentally different. We therefore first establish a generalized stability criterion for g-tempered fractional systems, and then apply it to derive stability results for the specific equilibrium points of our model.

7.1. General Local Stability Criterion

We first derive the characteristic equation governing the local asymptotic stability of an arbitrary equilibrium state $\mathbf{x}^*$ for a general delay-free g-tempered fractional system.

Theorem 5 (Stability criterion for linear g-tempered fractional systems)**.** *Let* $0 < \alpha < 1$, $\mu \geq 0$, *and let* $g \in C^1([a,\infty))$ *be strictly increasing, with* $g'(t) > 0$ *and*

$$\lim_{t\to\infty} g(t) = \infty.$$

Consider the linear g-tempered fractional system

$$ {}^{C}\mathcal{D}^{\alpha,\mu}_{a,g}\mathbf{Y}(t) = J\mathbf{Y}(t), \qquad t \geq a, \tag{21}$$

where $J \in \mathbb{C}^{m\times m}$ *is a constant matrix.*

Define

$$\Delta(s) := \det\Big(sI - (s+\mu)^{1-\alpha}J\Big), \tag{22}$$

where $(s+\mu)^{1-\alpha}$ *is taken with the principal branch in* $\mathbb{C}\setminus(-\infty,-\mu]$.

Then the zero solution of (21) *is asymptotically stable if and only if*

$$\Delta(s) \neq 0 \qquad \text{for every } s \in \mathbb{C}, \quad \operatorname{Re} s \geq 0. \tag{23}$$

Equivalently, if $\lambda_1,\dots,\lambda_m$ *are the eigenvalues of* J, *then asymptotic stability holds if and only if every solution of*

$$\frac{s}{(s+\mu)^{1-\alpha}} = \lambda_j, \qquad j = 1,\dots,m, \tag{24}$$

satisfies

$$\operatorname{Re} s < 0.$$

For $\mu = 0$, *condition* (24) *reduces to*

$$s^\alpha = \lambda_j,$$

and hence to the classical Matignon criterion

$$|\arg(\lambda_j)| > \frac{\alpha\pi}{2}, \qquad j = 1,\dots,m.$$

Proof. Introduce the new time variable

$$\tau = g(t) - g(a)$$

and define

$$\widetilde{\mathbf{Y}}(\tau) := \mathbf{Y}\Big(g^{-1}(\tau + g(a))\Big).$$

Since g is strictly increasing and $g(t) \to \infty$ as $t \to \infty$, we have

$$t \to \infty \quad \Longleftrightarrow \quad \tau \to \infty.$$

By the definition of the g-tempered Caputo derivative,

$$ {}^{C}\mathcal{D}^{\alpha,\mu}_{a,g}\mathbf{Y}(t) = \frac{1}{\Gamma(1-\alpha)}\int_a^t [g(t)-g(r)]^{-\alpha} e^{-\mu[g(t)-g(r)]}\mathbf{Y}'_g(r)\,dg(r),$$

where

$$\mathbf{Y}'_g(r) = \frac{d\mathbf{Y}}{dg(r)}.$$

After the above change in variables, this becomes

$${}^{C}\mathcal{D}^{\alpha,\mu}\widetilde{\mathbf{Y}}(\tau) = \frac{1}{\Gamma(1-\alpha)}\int_0^\tau (\tau-\xi)^{-\alpha} e^{-\mu(\tau-\xi)}\widetilde{\mathbf{Y}}'(\xi)\,d\xi.$$

Thus (21) is equivalent to

$${}^{C}\mathcal{D}^{\alpha,\mu}\widetilde{\mathbf{Y}}(\tau) = J\widetilde{\mathbf{Y}}(\tau).$$

Let

$$\widehat{\mathbf{Y}}(s) = \mathcal{L}\{\widetilde{\mathbf{Y}}\}(s).$$

Using

$$\mathcal{L}\left\{{}^{C}\mathcal{D}^{\alpha,\mu}\widetilde{\mathbf{Y}}\right\}(s) = (s+\mu)^{\alpha-1}\left[s\widehat{\mathbf{Y}}(s) - \widetilde{\mathbf{Y}}(0)\right],$$

we obtain

$$(s+\mu)^{\alpha-1}\left[s\widehat{\mathbf{Y}}(s) - \widetilde{\mathbf{Y}}(0)\right] = J\widehat{\mathbf{Y}}(s).$$

Hence

$$\left[sI - (s+\mu)^{1-\alpha}J\right]\widehat{\mathbf{Y}}(s) = \widetilde{\mathbf{Y}}(0),$$

and therefore

$$\widehat{\mathbf{Y}}(s) = \left[sI - (s+\mu)^{1-\alpha}J\right]^{-1}\widetilde{\mathbf{Y}}(0).$$

The singularities of the resolvent in $\mathbb{C}\setminus(-\infty,-\mu]$ are therefore determined by

$$\Delta(s) = 0.$$

Moreover, for $s \neq -\mu$,

$$\begin{aligned}\Delta(s) &= (s+\mu)^{m(1-\alpha)}\det\left(\frac{s}{(s+\mu)^{1-\alpha}}I - J\right)\\ &= (s+\mu)^{m(1-\alpha)}\prod_{j=1}^{m}\left(\frac{s}{(s+\mu)^{1-\alpha}} - \lambda_j\right).\end{aligned}$$

Consequently,

$$\Delta(s) = 0 \quad\Longleftrightarrow\quad \frac{s}{(s+\mu)^{1-\alpha}} = \lambda_j$$

for some $j \in \{1,\dots,m\}$.

If (23) holds, the resolvent has no singularity in the closed right half-plane. The branch point $s = -\mu$ and the associated branch cut $(-\infty,-\mu]$ are contained in the left half-plane when $\mu > 0$. Hence the inverse Laplace representation contains only decaying contributions, and

$$\widetilde{\mathbf{Y}}(\tau) \longrightarrow 0 \qquad \text{as } \tau \to \infty.$$

Therefore,

$$\mathbf{Y}(t) \longrightarrow 0 \qquad \text{as } t \to \infty,$$

because $\tau = g(t) - g(a) \to \infty$.

Conversely, if there exists a solution s_0 of (24) with $\operatorname{Re} s_0 > 0$, then the resolvent has a singularity in the open right half-plane. The corresponding inverse-Laplace contribution contains a non-decaying mode, and consequently

$$\widetilde{\mathbf{Y}}(\tau) \not\to 0.$$

Thus the zero solution is unstable. If a characteristic root satisfies $\operatorname{Re} s_0 = 0$, asymptotic stability also fails.

Finally, if $\mu = 0$, then

$$\frac{s}{(s+\mu)^{1-\alpha}} = s^{\alpha},$$

and the characteristic equation becomes

$$s^{\alpha} = \lambda_j.$$

All corresponding roots lie in the open left half-plane if and only if

$$|\arg(\lambda_j)| > \frac{\alpha\pi}{2},$$

which is the classical Matignon criterion. □

7.2. Disease-Free Equilibrium and Its Linearization

The disease-free equilibrium (DFE) is obtained by setting all fractional derivatives to zero and assuming no infections. This yields the following:

$$E_0 = \left(\frac{\Lambda}{\mu_0}, 0, 0, 0\right).$$

Indeed, all components are constant at E_0 and the g-derivative of a constant vanishes. Introduce the following perturbations:

$$S(t) = \frac{\Lambda}{\mu_0} + u_1(t), \qquad I(t) = u_2(t), \qquad Q(t) = u_3(t), \qquad R(t) = u_4(t).$$

The linearization of the system around E_0 is given by the following:

$$\begin{cases} {}^{C}\mathcal{D}^{\alpha,\mu}_{a,g} u_1(t) = -\mu_0 u_1(t) - \dfrac{\beta\Lambda}{\mu_0} u_2(t-\tau_1), \\ {}^{C}\mathcal{D}^{\alpha,\mu}_{a,g} u_2(t) = -(\sigma+\mu_0) u_2(t) + \dfrac{\beta\Lambda}{\mu_0} u_2(t-\tau_1), \\ {}^{C}\mathcal{D}^{\alpha,\mu}_{a,g} u_3(t) = -(\theta+\mu_0) u_3(t) + \sigma u_2(t-\tau_2), \\ {}^{C}\mathcal{D}^{\alpha,\mu}_{a,g} u_4(t) = -\mu_0 u_4(t) + \theta u_3(t-\tau_3). \end{cases}$$

The second equation is autonomous with respect to u_2. Consequently, once the behavior of u_2 is established, the remaining components can be treated successively.

7.3. Characteristic Equation for an Affine g

Analyzing the local stability of systems with arbitrary time-transformation $g(t)$ and delays is highly non-trivial in the frequency domain. However, the most important practical case allowing a direct spectral analysis is the affine transformation:

$$g(t) = at + b, \qquad a > 0.$$

Then

$$g(t) - g(s) = a(t-s),$$

and the transformation to the g-time scale is linear. Moreover, the explicit delay transforms neatly into the following:

$$g(t-\tau_i) = g(t) - a\tau_i.$$

Thus, a constant physical-time delay τ_i remains a constant delay in the transformed time scale, but with a rescaled length $a\tau_i$.

For the standard time scale $g(t) = t$ ($a = 1$), the characteristic symbol of our operator is

$$\Phi_{\alpha,\mu}(s) = s(s+\mu)^{\alpha-1},$$

where $\mu \geq 0$ is the tempering parameter. For the linearized SIQR system, evaluated at the disease-free equilibrium E_0, the characteristic determinant factorizes as follows:

$$\begin{aligned}\Delta(s) = &\left[\Phi_{\alpha,\mu}(s)+\mu_0\right]\left[\Phi_{\alpha,\mu}(s)+\mu_0\right]\left[\Phi_{\alpha,\mu}(s)+\theta+\mu_0\right]\\ &\times\left[\Phi_{\alpha,\mu}(s)+\sigma+\mu_0-\frac{\beta\Lambda}{\mu_0}e^{-s\tau_1}\right].\end{aligned} \tag{25}$$

For a general affine function $g(t) = at + b$, the exact same factorization holds after replacing each delay τ_i by its rescaled version $a\tau_i$.

7.4. A Basic Stability Property of the Characteristic Symbol

To analyze the roots of $\Delta(s) = 0$, the following elementary geometric property of the fractional symbol is crucial.

Lemma 6. *Let* $0 < \alpha < 1$ *and* $\mu \geq 0$. *If* $\operatorname{Re} s \geq 0$, *then*

$$\operatorname{Re}\left(s(s+\mu)^{\alpha-1}\right) \geq 0.$$

Moreover, for real $s \geq 0$, *the function* $\Phi_{\alpha,\mu}(s) = s(s+\mu)^{\alpha-1}$ *is nonnegative and strictly increasing for* $s > 0$.

Proof. Let $z = s + \mu$. Since $\operatorname{Re} s \geq 0$ and $\mu \geq 0$, we have $\operatorname{Re} z \geq 0$. Write z in polar form as follows:

$$z = re^{i\theta}, \qquad -\frac{\pi}{2} \leq \theta \leq \frac{\pi}{2}.$$

Since $s = z - \mu$ with $\mu \geq 0$, the argument of s lies between θ and the corresponding imaginary-axis direction. For $\theta \geq 0$,

$$0 \leq \arg(s) - (1-\alpha)\theta \leq \frac{\pi}{2},$$

and the case $\theta \leq 0$ follows by symmetry. Hence

$$\operatorname{Re}\left(sz^{\alpha-1}\right) = |s|\, r^{\alpha-1}\cos(\arg(s) + (\alpha-1)\theta) \geq 0.$$

Since $z = s + \mu$, we obtain $sz^{\alpha-1} = s(s+\mu)^{\alpha-1}$, which proves the first assertion.

For real $s \geq 0$, differentiation gives

$$\frac{d}{ds}\left[s(s+\mu)^{\alpha-1}\right] = (s+\mu)^{\alpha-2}\left(\mu+\alpha s\right) > 0$$

for $s > 0$. Thus the function is strictly increasing. □

7.5. Local Asymptotic Stability of the Disease-Free Equilibrium

We define the basic reproduction number for the g-tempered SIQR model by the following:

$$\mathcal{R}_0 = \frac{\beta\Lambda}{\mu_0(\sigma + \mu_0)}.$$

Theorem 6 (Local stability of the disease-free equilibrium)**.** *Assume $0 < \alpha < 1$ and $\mu \geq 0$. Let $g(t) = t$. Then the disease-free equilibrium E_0 is locally asymptotically stable if and only if*

$$\mathcal{R}_0 < 1.$$

The same result holds for any affine transformation $g(t) = at + b$ with $a > 0$. In particular, the stability condition is entirely independent of the time delays τ_1, τ_2, τ_3.

Proof. By (25), the characteristic roots are obtained from the roots of the scalar factors. The first three factors yield the following:

$$\Phi_{\alpha,\mu}(s) + \mu_0 = 0, \quad \Phi_{\alpha,\mu}(s) + \mu_0 = 0, \quad \Phi_{\alpha,\mu}(s) + \theta + \mu_0 = 0.$$

The roots determining the infection dynamics come from the final factor:

$$\Phi_{\alpha,\mu}(s) + \sigma + \mu_0 - \frac{\beta\Lambda}{\mu_0} e^{-s\tau_1} = 0. \tag{26}$$

Consider first any root s satisfying $\operatorname{Re} s \geq 0$. By Lemma 6, we know that $\operatorname{Re} \Phi_{\alpha,\mu}(s) \geq 0$. Since all parameters $\mu_0, \mu_0, \mu_0, \theta$ are strictly positive, it is immediately clear that $\Phi_{\alpha,\mu}(s) + \mu_0 \neq 0$, $\Phi_{\alpha,\mu}(s) + \mu_0 \neq 0$, and $\Phi_{\alpha,\mu}(s) + \theta + \mu_0 \neq 0$.

It remains to analyze (26). Let

$$b = \sigma + \mu_0, \qquad c = \frac{\beta\Lambda}{\mu_0}.$$

The condition $\mathcal{R}_0 < 1$ is equivalent to $c < b$. Suppose that s is a characteristic root with $\operatorname{Re} s \geq 0$. Since the real part of $\Phi_{\alpha,\mu}(s)$ is nonnegative, we have the following:

$$\left|\Phi_{\alpha,\mu}(s) + b\right| \geq b.$$

On the other hand, rearranging (26) gives the following:

$$\left|\Phi_{\alpha,\mu}(s) + b\right| = c\,|e^{-s\tau_1}| \leq c,$$

because $|e^{-s\tau_1}| = e^{-\operatorname{Re} s\,\tau_1} \leq 1$. Thus, we obtain the following:

$$b \leq \left|\Phi_{\alpha,\mu}(s) + b\right| \leq c < b,$$

which is a contradiction. Hence, all characteristic roots must satisfy $\operatorname{Re} s < 0$, meaning the disease-free equilibrium is locally asymptotically stable.

To prove necessity, suppose that $\mathcal{R}_0 > 1$, which implies $c > b$. For real $s \geq 0$, define the function

$$H(s) = \Phi_{\alpha,\mu}(s) + b - ce^{-s\tau_1}.$$

By Lemma 6, H is continuous on $[0, \infty)$ and

$$H(0) = b - c < 0.$$

Moreover, since $\alpha \in (0,1)$, $\lim_{s\to\infty} \Phi_{\alpha,\mu}(s) = \infty$, which means $\lim_{s\to\infty} H(s) = \infty$. By the intermediate value theorem, there exists at least one real root $s_* > 0$ such that $H(s_*) = 0$. This positive real root implies the equilibrium is unstable.

Finally, if $\mathcal{R}_0 = 1$, then $H(0) = 0$, meaning $s = 0$ is a characteristic root, and asymptotic stability fails. Consequently, $\mathcal{R}_0 < 1$ is both necessary and sufficient for local asymptotic stability.

For a general affine transformation $g(t) = at + b$, the delays are merely rescaled to $a\tau_i$, which modifies the exponential term to $e^{-sa\tau_1}$. Since $|e^{-sa\tau_1}| \leq 1$ for $\mathrm{Re}\, s \geq 0$, the exact same mathematical argument applies. □

7.6. Interpretation of the Stability Result

Theorem 6 is particularly useful because the tempering parameter μ and the fractional order α do not change the epidemic threshold for the disease-free equilibrium. They modify the temporal behavior of the solutions and the location of characteristic roots, but the threshold separating local stability from instability is still entirely determined by the following:

$$\mathcal{R}_0 = \frac{\beta\Lambda}{\mu_0(\sigma + \mu_0)}.$$

The delay τ_1 may affect the transient evolution and the distribution of the characteristic roots, but it cannot destabilize the disease-free equilibrium when $\mathcal{R}_0 < 1$. Conversely, for $\mathcal{R}_0 > 1$, the positive real characteristic root constructed in the proof shows that no choice of a finite nonnegative delay τ_1 can restore local asymptotic stability.

The delays τ_2 and τ_3 do not enter the characteristic factor determining the infectious component. They therefore do not change the local spectral stability of the disease-free equilibrium, although they may significantly alter the transient behavior of the quarantine and recovered compartments.

7.7. The Role of a General Nonlinear Function g

The preceding spectral analysis extends directly to affine functions g, but a fundamentally different situation arises for nonlinear g.

Let

$$\xi = g(t) - g(a), \qquad \widetilde{\mathbf{X}}(\xi) = \mathbf{X}(g^{-1}(\xi + g(a))).$$

For a constant physical-time delay τ_i, we have

$$\mathbf{X}(t - \tau_i) = \widetilde{\mathbf{X}}\Big(g(g^{-1}(\xi + g(a)) - \tau_i) - g(a)\Big).$$

Define the transformed delay function:

$$h_i(\xi) = g(g^{-1}(\xi + g(a)) - \tau_i) - g(a).$$

Then

$$\mathbf{X}(t - \tau_i) = \widetilde{\mathbf{X}}(h_i(\xi)).$$

If the transformation is affine, i.e., $g(t) = at + b$, then $h_i(\xi) = \xi - a\tau_i$. For a nonlinear g, however,

$$h_i(\xi) \neq \xi - c_i$$

in general. Thus, a constant physical-time delay maps to a *time-varying delay* in the transformed time scale. Consequently, the transformed SIQR system takes the form:

$${}^{C}\mathcal{D}^{\alpha,\mu}_{0,\mathrm{Id}}\widetilde{\mathbf{X}}(\xi) = F\Big(\widetilde{\mathbf{X}}(\xi), \widetilde{\mathbf{X}}(h_1(\xi)), \widetilde{\mathbf{X}}(h_2(\xi)), \widetilde{\mathbf{X}}(h_3(\xi))\Big),$$

where $\mathrm{Id}(t) = t$.

Remark 8. *For nonlinear g, a standard Laplace-transform characteristic equation containing the factors $e^{-s\tau_i}$ is not available. Indeed, the transform $\mathcal{L}\{\widetilde{\mathbf{X}}(h_i(\xi))\}$ cannot be represented as a simple scalar multiple of $\widetilde{\mathbf{X}}(s)$. Therefore, the exact spectral argument used in Theorem 6 is restricted to affine g. This is not merely a technical obstacle; it reflects the physical fact that a nonlinear g changes the temporal scale on which fractional memory is measured, simultaneously stretching and compressing the representation of physical delays on that scale.*

7.8. A Sufficient Condition for General Nonlinear g

For the general nonlinear g case, the integral representation provides the appropriate starting point for stability estimates. For the linearized system, it takes the following form:

$$\mathbf{u}(t) = \mathbf{u}(a) + \int_a^t q_{\alpha,\mu}\big(g(t) - g(s)\big) \times \left[A_0\mathbf{u}(s) + A_1\mathbf{u}(s-\tau_1) + A_2\mathbf{u}(s-\tau_2) + A_3\mathbf{u}(s-\tau_3)\right] dg(s),$$

where A_i are the respective Jacobian matrices and $q_{\alpha,\mu}$ is the resolvent kernel defined in (10).

The kernel $q_{\alpha,\mu}(u)$ is nonnegative. However, a crucial observation is that for $\mu > 0$, it does not have a finite total mass (it does not vanish at infinity). Indeed, evaluating the limit yields the following:

$$\lim_{u\to\infty} q_{\alpha,\mu}(u) = \mu^{1-\alpha}.$$

Therefore, a simple contraction mapping estimate based solely on the total mass of the resolvent kernel cannot yield an asymptotic stability criterion on an infinite interval.

This observation is mathematically significant: for the present definition of the g-tempered derivative, a delay-independent asymptotic stability criterion for arbitrary nonlinear g cannot be obtained by the same simple integral-kernel argument that might be available for standard Caputo operators or exponentially decaying kernels.

Instead, establishing stability for arbitrary nonlinear g requires advanced techniques such as fractional Lyapunov–Razumikhin or Lyapunov–Krasovskii functionals adapted to time-varying delays, or suitable comparison principles. Such approaches are consistent with recent stability results for tempered fractional systems with delays, which utilize generalized Grönwall, Jensen, and Hölder inequalities (see, for example, [52]).

7.9. Summary of the Qualitative Stability Results

The preceding analysis leads to several complementary conclusions regarding the g-tempered SIQR model with time delays. For the delay-free g-tempered fractional system, the characteristic equation is governed by the shifted fractional symbol $\Phi_{\alpha,\mu}(s) = s(s+\mu)^{\alpha-1}$, and the classical Matignon condition is recovered when $\mu = 0$. For the full SIQR model with $g(t) = t$, the characteristic equation factorizes and shows that only the infection delay τ_1 enters the local spectral stability condition at the disease-free equilibrium, while τ_2 and τ_3 affect only the transient dynamics of the quarantine and recovered compartments.

The condition $\mathcal{R}_0 < 1$ provides a simple, delay-independent criterion that is both necessary and sufficient for the local asymptotic stability of the disease-free equilibrium. Interestingly, neither the fractional order α nor the tempering parameter μ alters this fundamental epidemic threshold; instead, they shape the transient behavior, damping rates, and the distribution of the characteristic roots without shifting the stability boundary $\mathcal{R}_0 = 1$.

For a general nonlinear function g, the transformation of the fractional memory remains straightforward, but physical-time delays become time-varying delays on the transformed time scale. Consequently, a standard finite-dimensional characteristic equation is generally unavailable. In that setting, the Volterra integral formulation provides an alternative route to robust sufficient stability conditions. This distinction highlights the complementary roles of distributed fractional memory, tempering, and explicit time delays in the proposed epidemiological model.

Corollary 1 (Practical stability test)**.** *For $g(t) = t$ and $0 < \alpha < 1$, the local asymptotic stability of an arbitrary equilibrium P^* of the SIQR system can be investigated by computing the characteristic roots of*

$$\det\left[s(s+\mu)^{\alpha-1}I_4 - A_0 - A_1e^{-s\tau_1} - A_2e^{-s\tau_2} - A_3e^{-s\tau_3}\right] = 0.$$

The equilibrium is locally asymptotically stable provided that all characteristic roots satisfy

$$\operatorname{Re} s < 0.$$

Consequently, while the threshold $\mathcal{R}_0 < 1$ for the disease-free equilibrium is invariant under changes in α and μ, the transient dynamics, damping rates, and the stability regions of endemic equilibria are heavily influenced by these fractional and tempering parameters.

Remark 9 (Complementarity of fractional memory and delays)**.** *The preceding analysis also illustrates the deep complementarity of the two memory mechanisms considered in this paper. The fractional operator introduces a distributed memory effect, through which the past history contributes continuously to the present state via a power-law kernel modulated by tempering. The delay terms, in contrast, introduce specific, localized discrete temporal lags associated directly with the latency of infection, the transition to quarantine, or the recovery processes.*

These two mechanisms affect the characteristic equation in fundamentally different ways: the fractional parameters enter through the algebraic symbol function $s(s+\mu)^{\alpha-1}$, whereas the discrete delays enter through the exponential factors $e^{-s\tau_i}$.

Their simultaneous presence allows the mathematical model to accurately distinguish between continuous distributed memory and explicitly delayed biological responses. This provides a rigorous mathematical and epidemiological justification for retaining both mechanisms in tandem, rather than treating one as a redundant replacement for the other.

7.10. Sensitivity Analysis of the Basic Reproduction Number

To evaluate how variations in the epidemiological parameters affect disease transmission, we perform a sensitivity analysis on the basic reproduction number $\mathcal{R}_0$. Normalized sensitivity indices provide a convenient and standardized measure of the relative influence of each model parameter on $\mathcal{R}_0$.

For a given parameter p, the normalized forward sensitivity index is defined as follows:

$$\Upsilon_p^{\mathcal{R}_0} = \frac{\partial \mathcal{R}_0}{\partial p}\frac{p}{\mathcal{R}_0}. \tag{27}$$

A positive sensitivity index ($\Upsilon_p^{\mathcal{R}_0} > 0$) indicates that an increase in the parameter p leads to an increase in $\mathcal{R}_0$ (thus promoting disease spread), whereas a negative index indicates the opposite (inhibiting transmission).

Recall the basic reproduction number for our g-tempered SIQR model,

$$\mathcal{R}_0 = \frac{\beta\Lambda}{\mu_0(\sigma+\mu_0)}.$$

By applying definition (27) to each parameter appearing in $\mathcal{R}_0$, we obtain explicit analytical expressions for their relative impacts. The resulting normalized sensitivity indices are summarized in Tables 3 and 4.

Table 3. Normalized sensitivity indices of the basic reproduction number $\mathcal{R}_0$ with respect to the parameters of the SIQR model.

Parameter p	$\Upsilon_p^{\mathcal{R}_0}$	Effect on $\mathcal{R}_0$
β	$+1$	Positive proportional effect
Λ	$+1$	Positive proportional effect
μ_0	-1	Negative proportional effect
σ	$-\frac{\sigma}{\sigma+\mu_0}$	Negative effect
μ_0	$-\frac{\mu_0}{\sigma+\mu_0}$	Negative effect
θ	0	No direct effect
r	0	No direct effect
τ_1	0	No direct effect
τ_2	0	No direct effect
τ_3	0	No direct effect
α	0	No direct effect
μ	0	No direct effect
g	0	No direct effect

Table 4. Quantitative comparison of the untempered ($\mu = 0$) and tempered ($\mu = 0.05$) SIQR models for two choices of the time-scaling function g.

$g(t)$	Quantity	$\mu = 0$	$\mu = 0.05$
$g(t) = t$	$I(T)$	5.519203	2.617740
	$Q(T)$	3.462823	1.145862
	$R(T)$	1.241643	0.491273
	$\max I(t)$	5.519203	2.617740
	$\max Q(t)$	3.462823	1.145862
	$\int_0^T I(t)\,dt$	429.555523	238.090004
	$\int_0^T Q(t)\,dt$	234.139923	95.803480
$g(t) = \ln(1+t)$	$I(T)$	1.475850	1.118148
	$Q(T)$	0.229111	0.176058
	$R(T)$	0.073723	0.059277
	$\max I(t)$	1.475850	1.118148
	$\max Q(t)$	0.229111	0.176058
	$\int_0^T I(t)\,dt$	103.325271	80.652751
	$\int_0^T Q(t)\,dt$	16.027754	12.920698

Since

$$\mathcal{R}_0 = \frac{\beta\Lambda}{\mu_0(\sigma+\mu_0)},$$

the normalized sensitivity indices satisfy

$$\Upsilon_\beta^{\mathcal{R}_0} = \Upsilon_\Lambda^{\mathcal{R}_0} = 1, \qquad \Upsilon_{\mu_0}^{\mathcal{R}_0} = -1,$$

and

$$\Upsilon_\sigma^{\mathcal{R}_0} = -\frac{\sigma}{\sigma+\mu_0}, \qquad \Upsilon_{\mu_0}^{\mathcal{R}_0} = -\frac{\mu_0}{\sigma+\mu_0}.$$

All remaining model parameters have zero direct sensitivity because they do not appear explicitly in the expression for $\mathcal{R}_0$. In particular, the fractional-order parameter α,

the tempering parameter λ, the delays τ_1, τ_2, τ_3, and the time-transformation function g do not affect the threshold quantity $\mathcal{R}_0$ directly. Their influence may, however, be manifested in the transient dynamics and in the time evolution of the epidemic.

8. Numerical Simulations

Remark 10 (Numerical implementation and the method of steps)**.** *To visualize the impact of the generalized tempered fractional derivative, time-scaling functions $g(t)$, and explicit delays on the SIQR model, we implement a custom numerical solver. When applying the generalized fractional Adams–Bashforth–Moulton (ABM) predictor–corrector method (see, e.g., [53,54]), special care is required regarding numerical stability. In particular, when the fractional order α is small, the Predictor-Evaluate-Correct-Evaluate (PECE) iterative scheme can be sensitive ([30]). If the fractional predictor overshoots and the corrector fails to adequately stabilize it, the presence of discrete delays (τ_i) may induce artificial numerical oscillations or divergence. To circumvent this, the step size must be appropriately controlled for all values of α.*

A natural question that arises for delayed systems is why the classical method of steps is not utilized. For standard integer-order differential delay equations, the method of steps solves the equation sequentially over intervals $[0, \tau], [\tau, 2\tau], \ldots$ by using the historical state defined on $[-\tau, 0]$. However, this approach breaks down in fractional calculus because fractional derivatives are inherently nonlocal. The state at time t depends on the entire history from the initial time 0 to t via the memory kernel. Consequently, one cannot decouple the intervals or 'reset' the problem at $t = \tau$ in the traditional manner.

Instead, a global discrete convolution (integral sum) approach must be employed, accounting simultaneously for the continuous 'fractional memory' and the discrete 'delay memory.' From a modeling perspective, when α is small, the system exhibits heavy memory: the infection dynamics do not merely react to the state at $t - \tau$ but rather to a weighted cumulative history spanning back to $t = 0$. This introduces a temporal 'drag' that delays the initial outbreak while sustaining the infection for a significantly longer duration than in classical models.

For the numerical part, we employ a predictor–corrector scheme adapted from the numerical methodology developed in [30]. The simulations are used to illustrate the qualitative effects of the fractional order, tempering, delays, and the time-scaling function g on the epidemic dynamics. We emphasize that the present paper does not provide a new convergence or error analysis of the numerical scheme; a rigorous numerical analysis specifically tailored to the combined delayed g-tempered model is not complete and is left for a future paper.

Remark 11. *In order to visualize the impact of the generalized tempered fractional derivative and the scaling function $g(t)$ on the delayed SIQR model, the system must be solved numerically. As standard scientific (Python 3.9.2) libraries do not support generalized tempered fractional delay differential equations with arbitrary time-scaling functions g, we can implement a custom Volterra integral solver (see [19]). This method involves discretizing the equivalent integral representation established in (7):*

$$\mathbf{X}(t) = \mathbf{X}(0) + \int_0^t q_{\alpha,\mu}\big(g(t) - g(s)\big)\mathbf{F}(\mathbf{X}(s), \mathbf{X}(s-\tau_1), \mathbf{X}(s-\tau_2), \mathbf{X}(s-\tau_3))dg(s),$$

where the kernel $q_{\alpha,\mu}$ is given by (6).

The numerical results obtained here were produced using a modified Adams–Bashforth–Moulton predictor–corrector scheme [30], where past states at delayed arguments $s - \tau_i$ are evaluated via interpolation on the computed grid (see, e.g., [53,54] for the classical framework, and [30] for adaptations to g-tempered operators).

1. The case of $g(t) = t$ and a constant initial function (Figures 8–11).

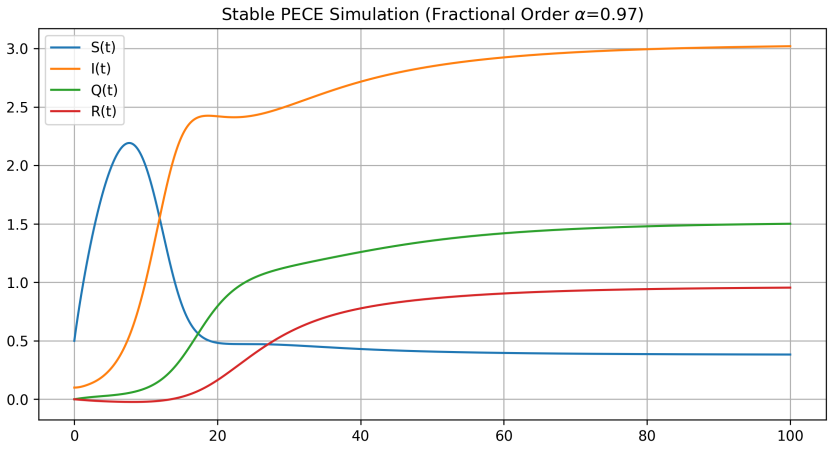

Figure 8. The linear case $g(t) = t$ with high order of derivatives: $\alpha = 0.97$.

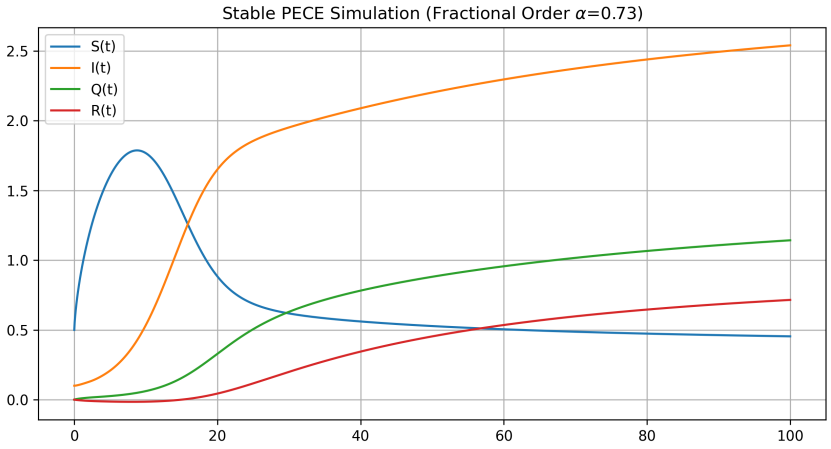

Figure 9. The linear case $g(t) = t$ with high order of derivatives: $\alpha = 0.73$.

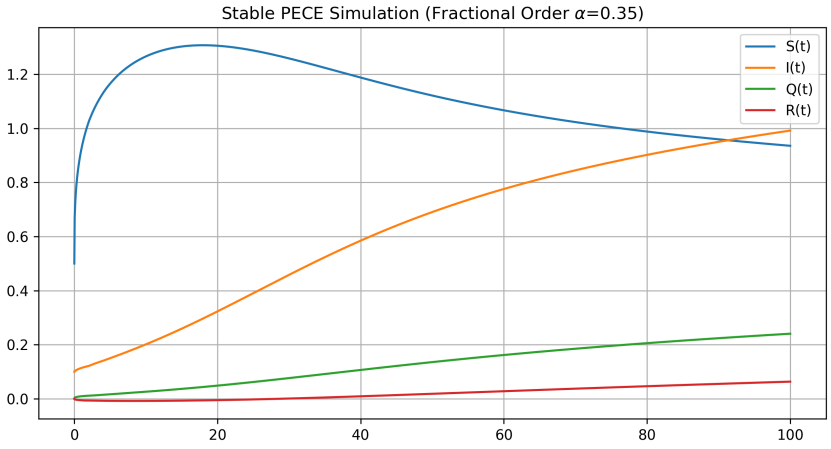

Figure 10. The linear case $g(t) = t$ with small order of derivatives: $\alpha = 0.35$.

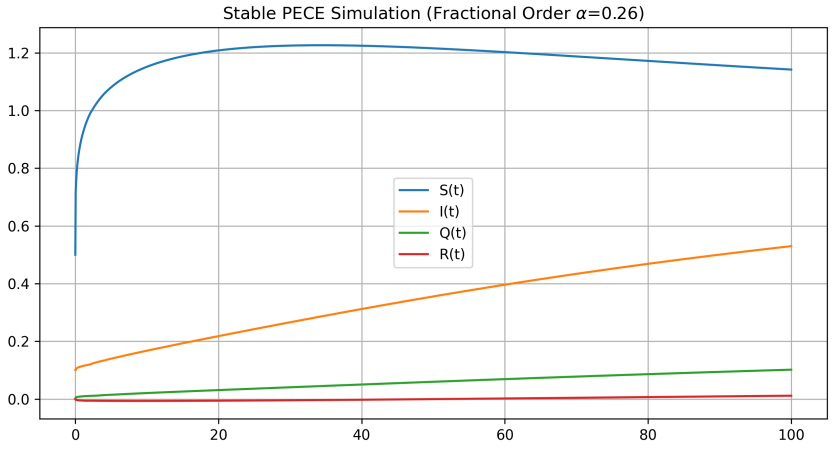

Figure 11. The linear case $g(t) = t$ with small order of derivatives: $\alpha = 0.26$.

2. The case of general g-derivative (the case of Hadamard-type derivatives) (Figures 12 and 13).

And now, here is a comparison of a few models with different sets of parameters (Figures 14 and 15): $[\Lambda, \beta, \mu_0, \sigma, \theta, r] = [0.6, 0.5, 0.05, 0.1, 0.1, 0.04]$. All the delay periods are fixed ($\tau = 2$). The value of the parameter $\alpha = 0.85$ is typical in epidemiological fractional models.

Based on the numerical simulations, we can draw the following key observations:

1. Invariance of the equilibrium state: The final steady state is independent of the choice of g. Models governed by different time-scaling functions eventually converge to the same unique equilibrium point E^*. This is a natural consequence of the fact that equilibrium states are determined by the algebraic condition $F(X^*) = 0$, which depends solely on the epidemiological parameters rather than on the memory operator or scaling function g.
2. Dependency of transient dynamics on g: While the destination (E^*) is invariant, the 'journey'—including the height of the epidemic peak, the time of its occurrence, and the overall damping rate—is heavily shaped by the choice of g, the fractional order α, and the tempering parameter μ.

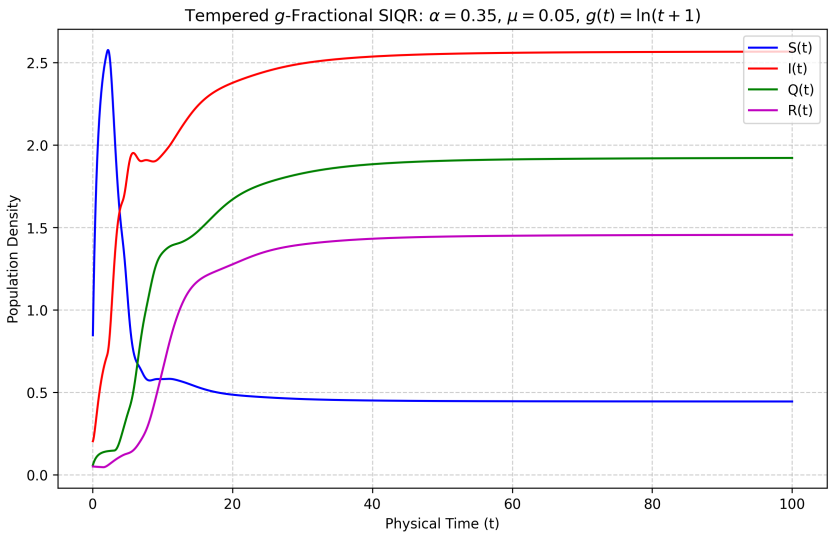

Figure 12. The nonlinear case $g(t) = \ln(t+1)$, $\mu = 0.05$ and $\alpha = 0.35$.

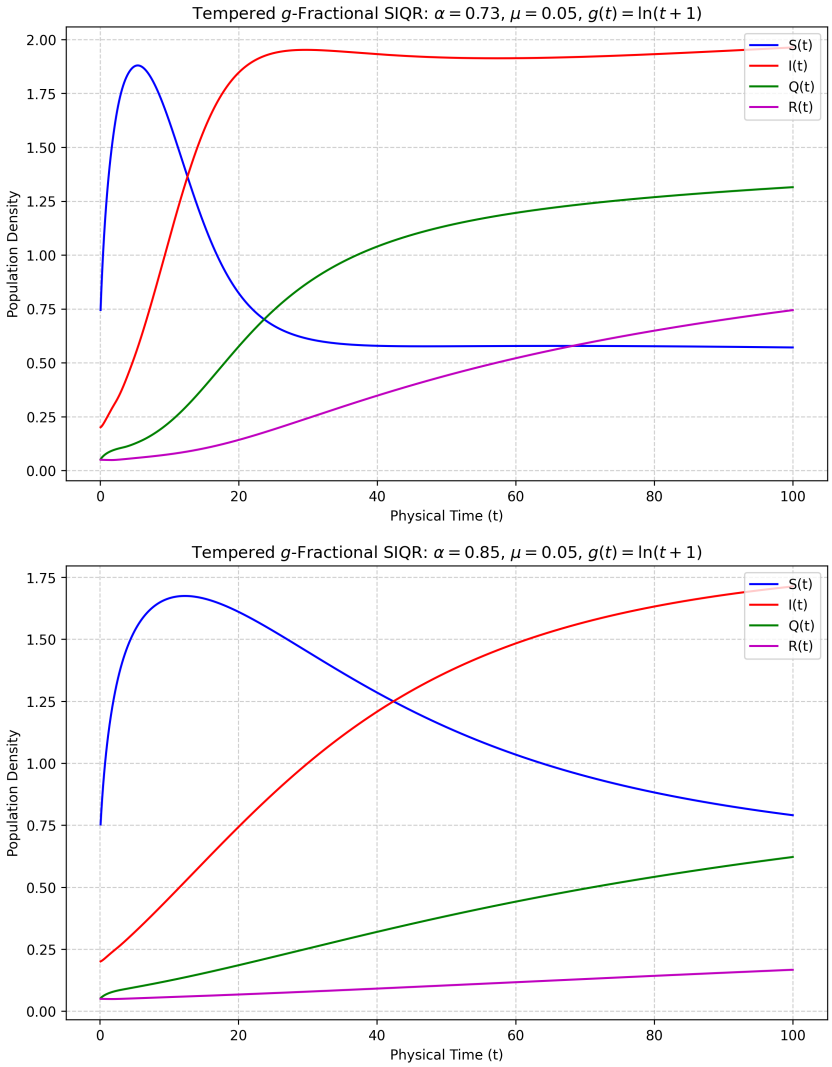

Figure 13. The nonlinear case $g(t) = \ln(t+1)$, $\mu = 0.005$ and different sets of parameters: $\alpha = 0.73$ and $\alpha = 0.85$.

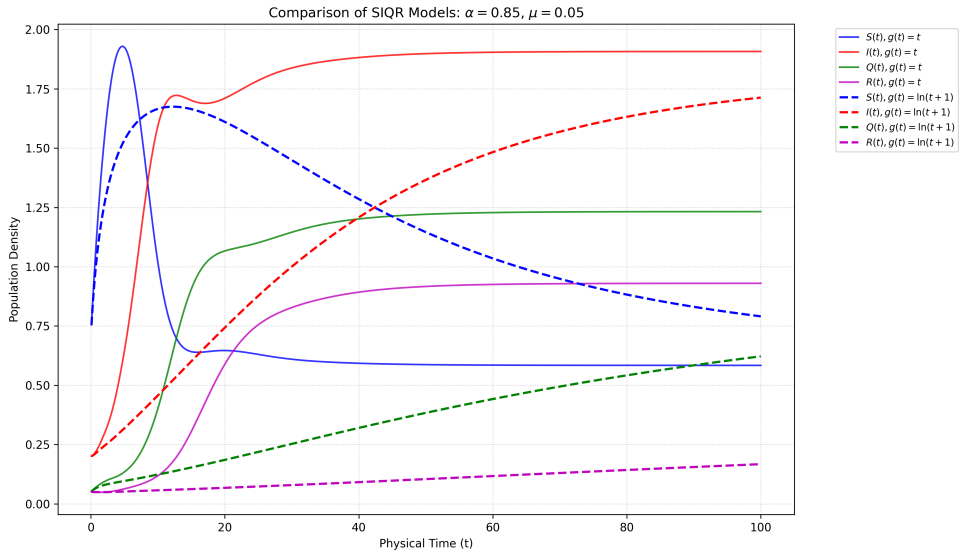

Figure 14. A comparison of selected simulations ($g(t) = t$ or $g(t) = \ln(1+t)$) of the epidemiological model. Untempered case: $\mu = 0$, $\alpha = 0.85$.

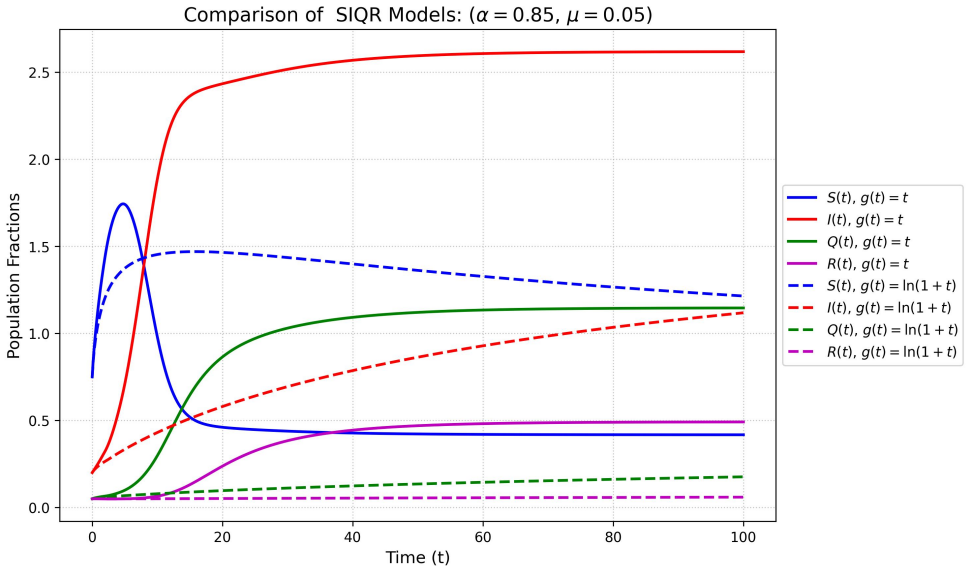

Figure 15. A comparison of selected simulations ($g(t) = t$ or $g(t) = \ln(1 + t)$) of the epidemiological model for $\alpha = 0.85$. Tempered case $\mu = 0.05$.

These simulations illustrate how the parameters of the generalized fractional derivative provide fine-grained control over the epidemic progression. Although such models are specifically tailored here for pathogens requiring quarantine (the SIQR framework), the proposed derivative framework possesses a much broader applicability to general epidemiological systems characterized by complex memory effects. Because analytical closed-form solutions are generally unavailable for nonlinear fractional models, relying on numerical simulations is indispensable. Furthermore, the inverse problem of determining fractional derivative parameters from observed data is notoriously ill-posed (see [29] for a detailed discussion within the SIQR context), necessitating robust numerical solvers. It is worth emphasizing that the custom numerical algorithms developed in this paper bridge this gap, enabling reliable simulation of g-tempered fractional systems with delays. For instance, utilizing the generalized fractional Adams–Bashforth–Moulton method [30] (with tempering parameter $\mu = 0$ in specific comparative runs), one can systematically explore how variations in the fractional order α reshape the epidemic curves over time (see Figures 16–19).

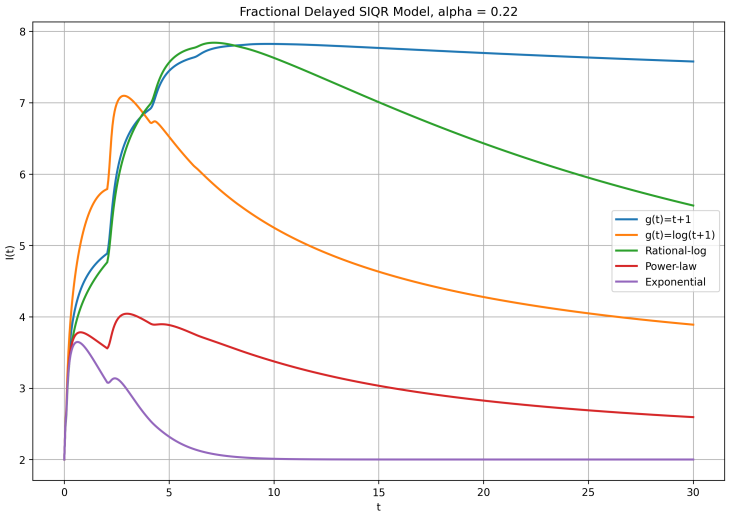

Figure 16. *Cont.*

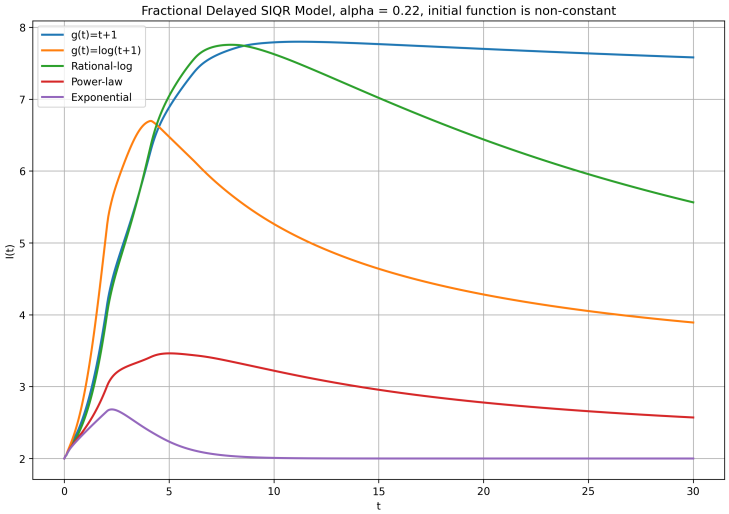

Figure 16. The impact of the time-tempering functions g on simulations for small parameter $\alpha = 0.22$ and $\mu = 0$. The set of functions g is discussed in Section 3.

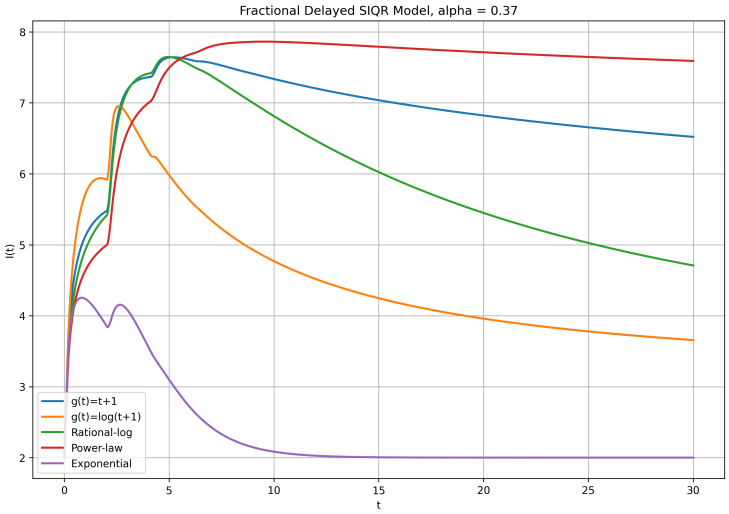

Figure 17. The impact of the different time-tempering functions g on simulations for the parameters $\alpha = 0.37$ and $\mu = 0$. The initial functions are constant.

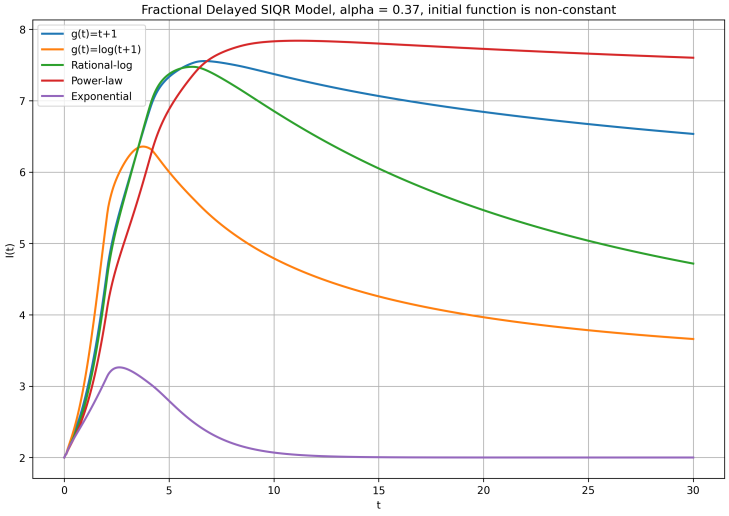

Figure 18. The impact of the different time-tempering functions g on simulations for the parameter $\alpha = 0.37$ and $\mu = 0$. The set of functions g is discussed in Section 3.

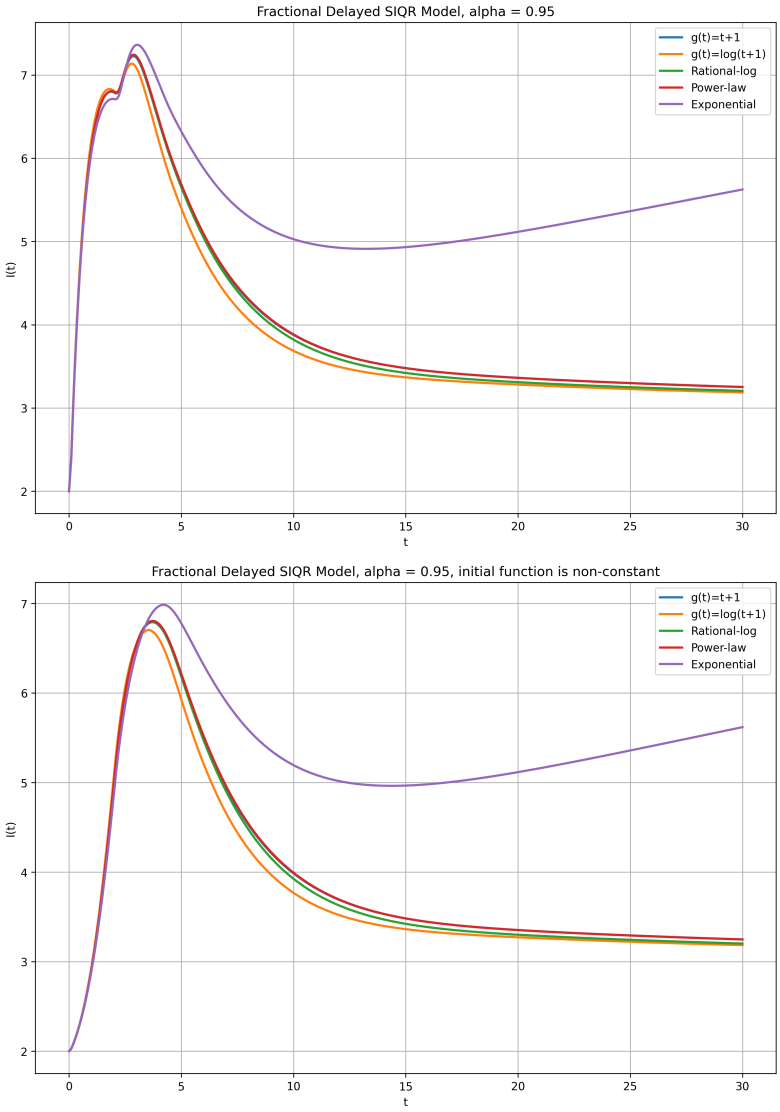

Figure 19. The impact of the time-tempering functions g on simulations for $\alpha = 0.95$ (close to 1), and $\mu = 0$.

9. Conclusions

In this paper, we introduced and rigorously analyzed a generalized g-tempered fractional SIQR epidemic model incorporating three distinct explicit time delays. The principal novelty of the model is the simultaneous treatment of tempered fractional memory and multiple epidemiological delays within a nonlinearly time-scaled framework.

The main theoretical and numerical contributions of this paper can be summarized as follows:

- Combined memory-delay framework: We formulated an SIQR epidemic model in which a g-tempered fractional derivative is coupled with three distinct time delays. This formulation allows continuous distributed memory effects and discrete epidemiological lags to be incorporated simultaneously.
- Well-posedness: We established the non-negativity of the solution compartments and proved global existence of solutions on $[a, \infty)$ by means of a dedicated continuation argument and Volterra–Gronwall-type estimates. In the concrete SIQR system, the required a priori estimates are obtained from the total population, thereby avoiding the global linear growth condition used in the abstract result.

- Stability and threshold analysis: We derived the corresponding characteristic equation and established the disease-free stability threshold for the affine time-scaling case. In particular,
$$\mathcal{R}_0 = \frac{\beta\Lambda}{\mu_0(\sigma + \mu_0)}$$
is independent of the fractional order α, the tempering parameter μ, and all three delays. Hence, these memory and delay parameters affect the transient behavior but do not shift the threshold $\mathcal{R}_0 = 1$ in the affine-g setting. This is one of the principal findings of the paper.
- Role of the time-scaling function g: We showed that affine choices of g preserve constant physical delays, whereas general nonlinear choices transform constant delays into time-dependent delays. For general nonlinear g, only a partial analytical result is obtained, and a complete stability analysis of the resulting time-varying-delay system remains an open problem.
- Numerical simulations: Numerical experiments illustrate the influence of the fractional order, tempering parameter, delays, and the time-scaling function on the transient epidemic dynamics. The predictor–corrector method used for the simulations follows the numerical methodology developed in [30]. In the present paper, we do not provide an independent convergence or error analysis of this numerical scheme.

The interpretation of the transient effects associated with α, μ, g, and the delays is subject to the identifiability limitations of the corresponding inverse problem. As established in [29], these parameters cannot, in general, be identified independently from epidemic observations without additional information, regularization, or prior constraints.

A limitation of the present analysis concerns the case of a general nonlinear time-scaling function g. As discussed in Section 7.8, only a partial analytical result is currently available in this setting, and a complete stability analysis for the resulting time-varying-delay problem remains open. Thus, the conclusions concerning the threshold and stability structure for nonlinear g should be understood within the scope of the results established in this paper.

Future research will focus on completing the analytical treatment of the nonlinear-g case, as well as addressing the inverse problem of parameter estimation using real-world epidemiological data and extending the current g-tempered framework to optimal control problems involving vaccination and quarantine strategies.

Author Contributions: Conceptualization, K.C. and M.C.; Methodology, M.C.; Software, M.C.; Validation, K.C. and M.C.; Formal Analysis, M.C.; Investigation, K.C. and M.C.; Resources, M.C.; Data Curation, M.C.; Writing Original Draft Preparation, K.C. and M.C.; Writing Review and Editing, M.C.; Visualization, M.C.; Supervision, M.C.; Project Administration, M.C.; Funding Acquisition, K.C. and M.C. All authors have read and agreed to the published version of the manuscript.

Funding: The author Kinga Cichoń was supported by the Poznan University of Technology under Grant no. 0213/SBAD/0124.

Data Availability Statement: The original contributions presented in the study are included in the article. Further inquiries can be directed to the corresponding author.

Conflicts of Interest: The authors declare no conflicts of interest.

References

1. Almeida, R. A Caputo fractional derivative of a function with respect to another function. *Commun. Nonlinear Sci. Numer. Simul.* **2017**, *44*, 460–481. https://doi.org/10.1016/j.cnsns.2016.09.006.
2. Meerschaert, M.; Sabzikar, F.; Chen, J. Tempered fractional calculus. *J. Comput. Phys.* **2015**, *293*, 14–28. https://doi.org/10.1016/j.jcp.2014.04.024.

3. Samko, S.G.; Kilbas, A.S.; Marichev, O.I. *Fractional Integrals and Derivatives: Theory and Applications*; Gordon Breach: Singapore, 1993.
4. Kilbas, A.A.; Srivastava, H.M.; Trujillo, J.J. *Theory and Applications of Fractional Differential Equations*; Elsevier: Amsterdam, The Netherlands, 2006.
5. Salem, H.A.H.; Cichoń, M. Analysis of tempered fractional calculus in Hölder and Orlicz spaces. *Symmetry* **2022**, *14*, 1581. https://doi.org/10.3390/sym14081581.
6. Webb, J.R.L. Initial value problems for Caputo fractional equations with singular nonlinearities. *Electron. J. Differ. Equ.* **2019**, *117*, 1–32.
7. Du, M.; Wang, Z.; Hu, H. Measuring memory with the order of fractional derivative. *Sci. Rep.* **2013**, *3*, 3431. https://doi.org/10.1038/srep03431.
8. Zhao, D.; Luo, M. Representations of acting processes and memory effects: General fractional derivative and its application to theory of heat conduction with finite wave speeds. *Appl. Math. Comput.* **2019**, *346*, 531–544. https://doi.org/10.1016/j.amc.2018.10.037.
9. Barros, L.C.D.; Lopes, M.M.; Pedro, F.S.; Esmi, E.; Santos, J.P.C.D.; Sánchez, D.E. The memory effect on fractional calculus: An application in the spread of COVID-19. *Comput. Appl. Math.* **2021**, *40*, 72. https://doi.org/10.1007/s40314-021-01456-z.
10. Saeedian, M.; Khalighi, M.; Azimi-Tafreshi, N.; Jafari, G.R.; Ausloos, M. Memory effects on epidemic evolution: The susceptible-infected-recovered epidemic model. *Phys. Rev. E* **2017**, *95*, 022409. https://doi.org/10.1103/PhysRevE.95.022409.
11. Malathy, R.; Krishnan, G.S.S.; Loganathan, K. A Caputo fractional-order SEIHRD model for Ebola: Theoretical analysis, sensitivity, bifurcation, and numerical simulations. *Sci. Rep.* **2026**, *16*, 13661. https://doi.org/10.1038/s41598-026-42467-2.
12. Tarasov, V.E.; Tarasova, V.V. *Economic Dynamics with Memory: Fractional Calculus Approach*; Walter de Gruyter GmbH: Berlin, Germany, 2021; Volume 8.
13. Rajak, A.K. Nilam: A fractional-order epidemic model with quarantine class and nonmonotonic incidence: Modeling and simulations. *Iran. J. Sci. Technol. Trans. A Sci.* **2022**, *46.4*, 1249–1263. https://doi.org/10.1007/s40995-022-01339-w.
14. Lu, H.; Ding, Y.; Gong, S.; Wang, S. Mathematical modeling and dynamic analysis of SIQR model with delay for pandemic COVID-19. *Math. Biosci. Eng.* **2021**, *18*, 3197–3321. https://doi.org/10.3934/mbe.2021159.
15. Arino, J.; Van Den Driessche, P. Time delays in epidemic models. In *Delay Differential Equations and Applications*; Springer: Berlin/Heidelberg, Germany, 2006; pp. 539–578.
16. Zhai, S.; Luo, G.; Huang, T.; Wang, X.; Tao, J.; Zhou, P. Vaccination control of an epidemic model with time delay and its application to COVID-19. *Nonlinear Dyn.* **2021**, *106*, 1279–1292. https://doi.org/10.1007/s11071-021-06533-w.
17. Dell'Anna, L. Solvable delay model for epidemic spreading: The case of Covid-19 in Italy. *Sci. Rep.* **2020**, *10*, 15763. https://doi.org/10.1038/s41598-020-72529-y.
18. Rihan, F.A.; Kandasamy, U.; Alsakaji, H.J.; Sottocornola, N. Dynamics of a fractional-order delayed model of COVID-19 with vaccination efficacy. *Vaccines* **2023**, *11*, 758. https://doi.org/10.3390/vaccines11040758.
19. Cichoń, M.; Cichoń, K. On mathematical models based on delay differential equations in epidemiology. *Appl. Sci.* **2025**, *15*, 10267. https://doi.org/10.3390/app151810267.
20. Xu, S.; Hu, Y. Dynamic analysis of a Caputo fractional-order SEIR model with a general incidence rate. *Sci. Rep.* **2025**, *15*, 17561. https://doi.org/10.1038/s41598-025-01400-9.
21. D'Onofrio, A. Stability properties of pulse vaccination strategy in SEIR epidemic model. *Math. Biosci.* **2002**, *179*, 57–72. https://doi.org/10.1016/S0025-5564(02)00095-0.
22. Singh, J.P.; Kumar, S.; Baleanu, D.; Nisar, K.S. Monkeypox viral transmission dynamics and fractional-order modeling with vaccination intervention. *Fractals* **2023**, *31*, 2340096. https://doi.org/10.1142/S0218348X23400960.
23. Wenzel, J. Origins of SARS-CoV-1 and SARS-CoV-2 are often poorly explored in leading publications. *Cladistics* **2020**, *36*, 374–379. https://doi.org/10.1111/cla.12425.
24. Area, I.; Batarfi, H.; Losada, J.; Nieto, J.J.; Shammakh, W.; Torres, A. On a fractional order Ebola epidemic model. *Adv. Differ. Equ.* **2025**, *2015*, 278. https://doi.org/10.1186/s13662-015-0613-5.
25. Ain, Q.T.; Anjum, N.; Din, A.; Zeb, A.; Djilali, S.; Khan, Z.A. On the analysis of Caputo fractional order dynamics of Middle East Lungs Coronavirus (MERS-CoV) model. *Alex. Eng. J.* **2022**, *61*, 5123–5131. https://doi.org/10.1016/j.aej.2021.10.016.
26. Yaagoub, Z.; Farah, E.M.; Ahmad, S. Three-strain epidemic model for influenza virus involving fractional derivative and treatment. *J. Appl. Math. Comp.* **2025**, *71*, 1247–1266. https://doi.org/10.1007/s12190-024-02284-0.
27. Kermack, W.O.; McKendrick, A.G. A contribution to the mathematical theory of epidemics. *Proc. R. Soc. Lond. Ser. A* **1927**, *115*, 700–721.
28. Martcheva, M. *An Introduction to Mathematical Epidemiology*; Springer: New York, NY, USA, 2015; Volume 61.
29. Cichoń, M.; Cichoń, K. Fractional epidemic modeling: Theoretical constructions and estimation strategies. *Appl. Sci.* **2026**, *16*, 5347. https://doi.org/10.3390/app16115347.
30. Cichoń, M.; Cichoń, K. On numerical methods for g-tempered fractional differential equations with applications. *Mathematics* **2026**, *14*, 2458. https://doi.org/10.3390/math14142458.
31. Fahad, H.M.; Fernandez, A.; Rehman, M.U.; Siddiqi, M. Tempered and Hadamard-type fractional calculus with respect to functions. *Mediterr. J. Math.* **2021**, *18.4*, 143. https://doi.org/10.1007/s00009-021-01783-9.

32. Hethcote, H.W.; Stech, H.W.; van den Driessche, P. Periodicity and stability in epidemic models: A survey. In *Differential Equations and Applications in Ecology, Epidemics, and Population Problems*; Busenberg, S., Cooke, K.L., Eds.; Academic Press: New York, NY, USA, 1981; pp. 65–82.
33. Ma, Z.; Li, J. *Dynamical Modeling and Analysis of Epidemics*; World Scientific: Singapore, 2009.
34. Hoang, M.T.; Ehrhardt, M. Differential equation models for infectious diseases: Mathematical modeling, qualitative analysis, numerical methods and applications. *SeMA J.* **2026**, *83*, 435–470.
35. Rihan, F.A. *Delay Differential Equations and Applications to Biology*; Springer: Singapore, 2021.
36. Arino, O.; Hbid, M.L.; Dads, E.A. (Eds.) Delay Differential Equations and Applications. In *Proceedings of the NATO Advanced Study Institute Held in Marrakech, Morocco, 9–21 September 2002*; Springer Science and Business Media: Berlin/Heidelberg, Germany, 2007; Volume 205.
37. Wu, W.; Zhou, J.; Li, Z.; Tan, X. The effect of time delay on the dynamics of a fractional-order epidemic model. *Adv. Contin. Discret. Model.* **2025**, *2025*, 9. https://doi.org/10.1186/s13662-025-03868-1.
38. Cichoń, K.; Cichoń, M. On generalized fractional operators and related function spaces with applications. *Phys. D* **2024**, *465*, 134212. https://doi.org/10.1016/j.physd.2024.134212.
39. Deng, W.; Li, B.; Tian, W.; Zhang, P. Boundary problems for the fractional and tempered fractional operators. *Multiscale Model. Simul.* **2018**, *16*, 125–149. https://doi.org/10.1137/17M1116222.
40. Mali, A.D.; Kucche, K.D.; Fernandez, A.; Fahad, H.M. On tempered fractional calculus with respect to functions and the associated fractional differential equations. *Math. Meth. Appl. Sci.* **2022**, *45*, 11134–11157. https://doi.org/10.1002/mma.8441.
41. Guo, L.; Zhang, B.; Li, C. The controllability for the tempered fractional-order equation subjected to nonlocal delay and impulsive conditions. *Indian J. Pure Appl. Math.* **2026**, *33*, 1–20. https://doi.org/10.1007/s13226-026-00941-7.
42. Kosztołowicz, T.; Dutkiewicz, A. Subdiffusion equation with Caputo fractional derivative with respect to another function. *Phys. Rev. E* **2021**, *104*, 014118. https://doi.org/10.1103/PhysRevE.104.014118.
43. Sneddon, I.N. The use in mathematical physics of Erdélyi-Kober operators and of some of their generalizations. In *Fractional Calculus and Its Applications*; Springer: Berlin/Heidelberg, Germany, 2006.
44. Luchko, Y. General fractional integrals and derivatives and their applications. *Phys. D* **2023**, *455*, 133906. https://doi.org/10.1016/j.physd.2023.133906.
45. Hilfer, R. (Ed.) *Applications of Fractional Calculus in Physics*; World Scientific: Singapore, 2000.
46. Katugampola, U.N. New approach to a generalized fractional integral. *Appl. Math. Comput.* **2011**, *218*, 860–865. https://doi.org/10.1016/j.amc.2011.03.062.
47. Uchaikin, V.V. *Fractional Derivatives for Physicists and Engineers*; Springer: Berlin, Germany, 2013; Volume 2.
48. Paul, S.; Mahata, A.; Mukherjee, S.; Roy, B. Dynamics of SIQR epidemic model with fractional order derivative. *Partial Differ. Equ. Appl. Math.* **2022**, *5*, 100216. https://doi.org/10.1016/j.padiff.2021.100216.
49. Samanta, G.P. Permanence and extinction of a nonautonomous HIV/AIDS epidemic model with distributed time delay. *Nonlinear Anal.-Real. World Appl.* **2011**, *12*, 1163–1177. https://doi.org/10.1016/j.nonrwa.2010.09.010.
50. Delavari, H.; Baleanu, D.; Sadati, J. Stability analysis of Caputo fractional-order nonlinear systems revisited. *Nonlinear Dyn.* **2012**, *67*, 2433–2439. https://doi.org/10.1007/s11071-011-0157-5.
51. Matignon, D. Stability results for fractional differential equations with applications to control processing. *Comput. Engin. Syst. Appl.* **1996**, *2*, 963–968.
52. Medved', M.; Brestovanská, E. Differential equations with tempered ψ-Caputo fractional derivative. *Math. Model. Anal.* **2021**, *26*, 631–650. https://doi.org/10.3846/mma.2021.13252.
53. Diethelm, K.; Neville, J.; Ford, J.; Freed, A.D. Detailed error analysis for a fractional Adams method. *Numer. Algorithms* **2004**, *36*, 31–52. https://doi.org/10.1023/B:NUMA.0000027736.85078.be.
54. Wang, Z. A numerical method for delayed fractional-order differential equations. *J. Appl. Math.* **2013**, *2013.1*, 256071. https://doi.org/10.1155/2013/256071.